Surface engineering and the application of laser-based processes to stents - A review of the latest development

J. Dong [a], M. Pacella [a,*], Y. Liu [a,b], L. Zhao [a]

[a] Wolfson School of Mechanical, Electrical and Manufacturing Engineering, Loughborough University, Loughborough, Leicestershire, LE11 3TU, UK
[b] Centre for Biological Engineering, Loughborough University, Loughborough, Leicestershire, LE11 3TU, UK

A R T I C L E   I N F O

A B S T R A C T

Late in-stent thrombus and restenosis still represent two major challenges in stents' design. Surface treatment of stent is attracting attention due to the increasing importance of stenting intervention for coronary artery diseases. Several surface engineering techniques have been utilised to improve the biological response *in vivo* on a wide range of biomedical devices. As a tailorable, precise, and ultra-fast process, laser surface engineering offers the potential to treat stent materials and fabricate various 3D textures, including grooves, pillars, nanowires, porous and freeform structures, while also modifying surface chemistry through nitridation, oxidation and coatings. Laser-based processes can reduce the biodegradable materials' degradation rate, offering many advantages to improve stents' performance, such as increased endothelialisation rate, prohibition of SMC proliferation, reduced platelet adhesion and controlled corrosion and degradation. Nowadays, adequate research has been conducted on laser surface texturing and surface chemistry modification. Laser texturing on commercial stents has been also investigated and a promotion of performance of laser-textured stents has been proved.

In this critical review, the influence of surface texture and surface chemistry on stents performance is firstly reviewed to understand the surface characteristics of stents required to facilitate cellular response. This is followed by the explicit illustration of laser surface engineering of stents and/or related materials. Laser induced periodic surface structure (LIPSS) on stent materials is then explored, and finally the application of laser surface modification techniques on latest generation of stent devices is highlighted to provide future trends and research direction on laser surface engineering of stents.

1. Introduction

Nowadays, stenting is becoming a standard therapy for coronary artery diseases which are the number one cause of death worldwide every year. On one hand, extensive research has been carried out to improve stents performance by developing new alloy and polymer materials. But stents, including bare metal, drug eluting and biodegradable stents, still face many clinical challenges, such as in-stent thrombosis and restenosis. These problems are particularly important for biodegradable polymer stents [1], which showed increased rate of major adverse cardiac events [2,3] according to clinical data. On the other hand, surface modifications of topographic features and chemistry are important methods to improve the stents performance.

Surface modification techniques, such as sandblasting, chemical etching, and plasma-based techniques, have been developed for decades and applied to a range of biomedical devices. Sandblasting and chemical etching are two economic and easy to access techniques. They are both compatible with relatively large biomedical components. The rough surface fabricated by sandblasting provides a great performance for orthopaedic and dental biomedical devices [4–6]. However, sandblasting is a non-selective surface treatment method and most importantly, the residues from abrasive material are commonly observed from sandblasted samples [7,8], and some particles such as alumina residue are harmful for human health [9]. Chemical etching is another method to fabricate rough surfaces, and it usually produces porous surface on metallic materials but could also modify polymers such as polyether ether ketone (PEEK) [10] and poly (L-lactide) (PLLA) [11]. The accompanied chemistry modification in chemical etching sometimes provides advantages for biomedical devices such as anti-bacterial and anti-infective properties [12]. But sometimes the chemical residues could also cause problems, and for example fluoride produced by

---

Abbreviations

BAEC	bovine aortic endothelial cell
BDS	biodegradable stent
BMS	bare metal stent
CVD	chemical vapour deposition
DES	drug eluting stent
DLC	diamond-like carbon
DLIP	direct laser interference patterning
DRIE	deep reactive ion etching
DSC	differential scanning calorimetry
EC	endothelial cell
FTIR	Fourier Transform Infrared Spectroscopy
GPC	gel permeation chromatography
GPx	glutathione peroxidase
HAEC	human aortic endothelial cell
HAp	hydroxyapatite
HASMC	human aortic smooth muscle cell
HCAEC	human coronary artery endothelial cell
HCASMC	human coronary artery smooth muscle cell
HD	high density
HDMEC	human dermal microvascular endothelial cell
HF	hydrofluoric acid
HFC	human fibroblast cell
HUVEC	human umbilical vein endothelial cell
HUVSMC	human umbilical vein smooth muscle cell
ISR	in-stent restenosis
LCVD	laser chemical vapour deposition
LD	low density
LGN	laser gas nitridation
LIPSS	laser induced periodic surface structures
LST	late-stent thrombus
MD	medium density
NHDF	normal human dermal fibroblasts
NO	nitrogen oxide
PBMA	poly (n-butyl methacrylate)
PCL	polycaprolactone
PDMS	poly (dimethyl siloxane)
PEEK	polyether ether ketone
PEG	polyethylene glycol
PEVA	polyethylene-co-vinyl acetate
PLD	pulsed laser deposition
PLGA	poly (lactic-co-glycolic acid)
PLLA	poly(ʟ-lactide)
PTFE	polytetrafluoroethylene
PU	polyurethane
PUU	polyether(urethane urea)
RAEC	rat aortic endothelial cell
RF plasma	radiofrequency plasmas
RMS	root mean square
SeDPA	3,3-diselenodipropionic acid
SEM	scanning electron microscope
SIBS	poly(styrene-b-isobutylene-b-styrene)
SiC	silicon carbide
SMC	smooth muscle cell
SNAP	S-Nitroso-N-acetyl-d-penicillamine
SS	stainless steel
TIDE	titanium inductively coupled plasma deep etch
TiNOX	titanium-nitride-oxide
VSMC	vascular smooth muscle cell
WAXS	Wide-angle X-ray scattering
XPS	X-ray photoelectron spectroscopy

hydrofluoric acid (HF) used in chemical etching can potentially damage DNA [13]. Another drawback of chemical etching is that it is generally non-selective. Selective etching could be achieved through masks and selective infiltration etching [14], but the process then becomes more complex and costly due to the increase of processing steps,. Plasma and laser-based techniques are two additional types of surface treatments with a wide range of surface modification abilities, particularly useful to improve the performance of materials used in biomedical applications. They both have the ability for surface texturing, chemistry modification, functionalisation, roughening and coating [15,16]. Both processes are also contactless and have demonstrated to be effective and reliable to achieve repeatable surface modifications. Plasma is a useful technique for biomedical device applications, such as stents [17], bone-implants [18] and anti-biofilms [19]. Although plasma techniques can easily roughen the target material, freeform textures (e.g. nanopillar and porous surfaces) would require more control and precision through complex experiment set-up such as radiofrequency plasma [20] or masking processes [21]. But for laser processing, highly repeatable surface textures and freeform texture designs can be achieved through interference patterning and polarised lasers [22,23]. Laser-based processes provide a larger range for texture design (from nano to micron scale) combined with surface chemistry modification capability. Furthermore, lasers have been successfully employed to texture curved surfaces [24]. Hence, this efficient, highly tailorable and precise technique could be applied to stents surface modification.

Laser surface modification of stents is still a novel area, but the latest developments in laser technology is starting to demonstrate some unique advantages especially for stent surface modifications. Therefore, it is important to understand the function of different surface textures and surface chemistry on stent cellular response and performance in order to harness the power of laser surface engineering of stent.

2. Effects of topography and surface chemistry on stents

The two main clinical problems for stenting therapy are late-stent thrombus (LST) and in-stent restenosis (ISR). And they are original from the implantation process of stents. Expanding the artery during stent percutaneous transluminal angioplasty, leading to the de-endothelialisation, deep arterial injury and stretching [25]. On one hand, the injury of endothelial cells (EC) layer combined with the effect of deep artery injury leads to inflammation, platelet degranulation and coagulation, and thrombosis [26]. On the other hand, the external stimulation from stents materials also induces the proliferation and migration of smooth muscle cells (SMCs). As a result, the stimulation of SMCs and macrophages make the formation of intimal hyperplasia. Combined with the recovery of elastic stretching, treated coronary artery becomes narrow again and ISR happens [27]. Effort to improve the efficiency of stent therapy has been going on for decades. From the early generation of bare mental stents (BMS), drug eluting stents (DES) to biodegradable stents (BDS), various of materials [28–33] and surface coatings [30,34–36] have been investigated together with surface texturing and surface chemistry modifications to improve the stents performance and reduce ISR and LST rate.,.

2.1. Influence of topographic features on stents performance

Texturing is a key surface modification method for biomedical devices/surfaces because the materials-cells interaction is largely affected by surface morphology and their mechanical properties. The influence of different textures varies according to different types of cells and extent, types and scales of topographic textures. It is crucial to understand the stimuli of surface topography to endothelial cells, smooth muscle cells and platelets for stents application because these three types

of cells have a vital role for restenosis and formation of in-stent thrombus. Common surface structures investigated for stents applications includes randomly roughened surface structures, grooved, tubular, porous structures, wired and spaghetti-like structures and combined hierarchical structures. Laser-based processing of stents is proved successful to produce grooved and spotted structures from micron to nano scale, randomly roughened structures [37], pillar [38] and porous structures [39]. Pulsed-laser deposition can also produce nanowire structures [40]. Additionally, 3D freeform surface structures can also be achieved by polarised laser [41]. These structures are not only able to be fabricated by laser, but also common surface structure investigated for

stent applications through other surface texturing techniques. The influence of textures on cells behaviour is universal regardless fabrication process, thus it is worth to review the biological influence of these textures fabricated by various surface texturing process.

2.1.1. Effects of surface roughness on adhesion cells of blood vessels

It is interesting that a random surface roughening process can provide a functional stents surface. Surface roughness can be modified through various surface treatment techniques such as blasting, grinding, plasma and laser treatments, and the modified roughness can be varied from nanoscale to macro-scale. It is noticed that the cellular response is
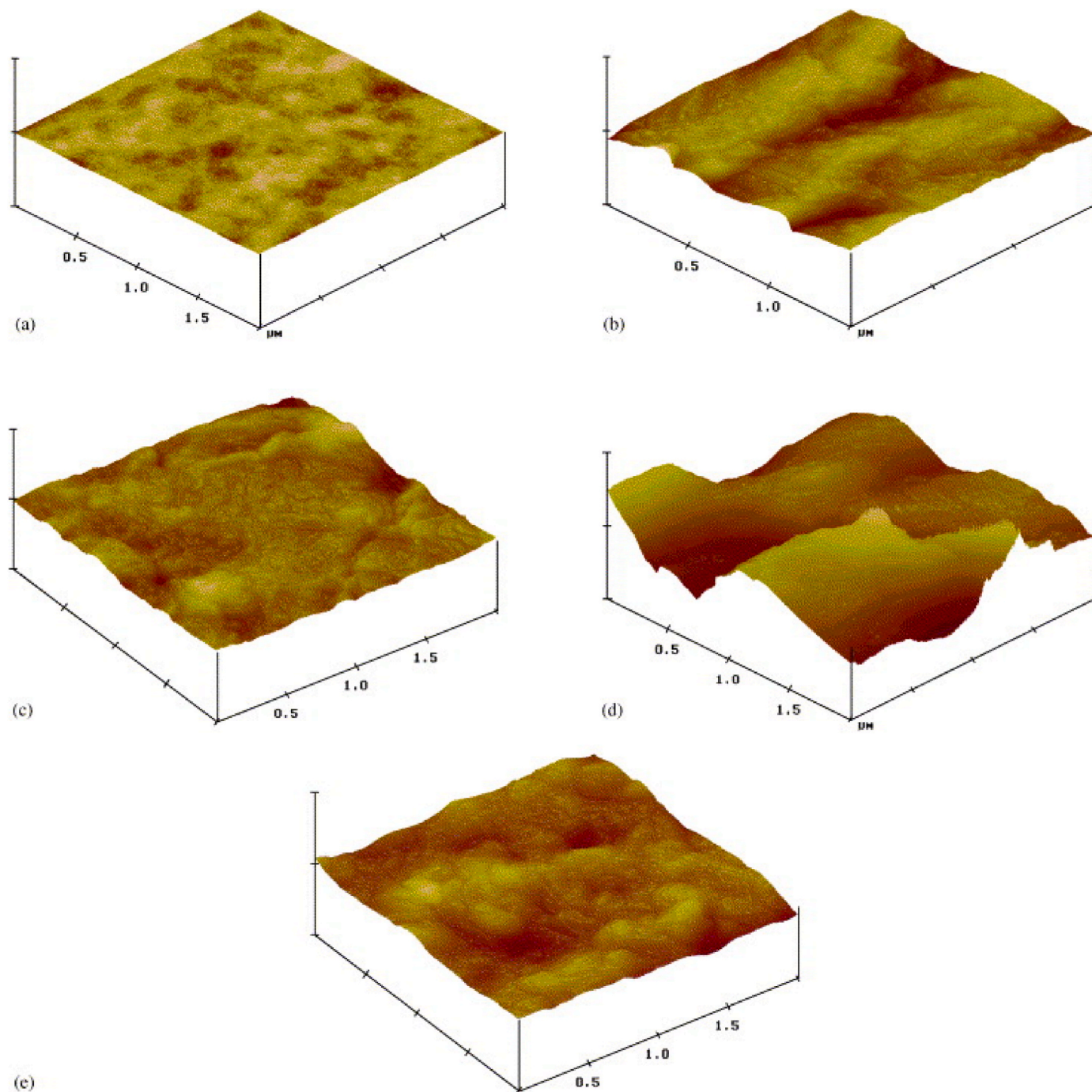

Fig. 1. AFM images of five surface with different roughness made by Chung et al. [44]: (a) PU surface, Ra: 1.53 ± 0.20 nm; (b) PU-PEG (2000 PEG length) surface, Ra: 20.10 ± 7.87 nm;(c) PU-PEG (mixing PEG length) surface, Ra: 39.79 ± 10.48 nm; (d) PU-PEG (mixing PEG length) surface coated with peptide, Ra: 18.63 ± 5.30 nm;(e) PU-PEG (mixing PEG length) surface coated with peptide, Ra: 34.58 ± 9.89 nm.

different depending on the types, size and morphology of cells, and furthermore this is also affected by the extent and geometry of surface roughness [42]. Hence, it is worth to review the response of ECs, SMCs and platelets to surfaces with different roughness, allowing evaluation of the influence of randomly roughened surfaces on biological response.

Adhesion and migration of ECs could be promoted on surface with nano-to micro-scale roughness. Various surface roughnesses had been achieved on pure Ti through electron beam deposition by Lu et al. [43]. In their study, samples with RMS roughness varied from 0.4 nm to 14 nm were tested using the rat aortic endothelial cells (RAEC) for EC adhesion, proliferation, and migration. EC increased adhesion cell density and migration ability on surface with higher RMS roughness. A similar trend was also found on some polymeric materials. Chung et al. [44] fabricated different PU-PEG surface with surface roughness Ra from 1.5 nm to 40 nm by grafting of PEG on to PU, and coated Gly–Arg–Gly–Asp peptide on the surface by photochemical technique to obtain different surface morphology (Fig. 1). Although peptide promoted adhesion of EC, the increasing of surface roughness also enhanced the EC adhesion and proliferation. The increasing of surface roughness in nanoscale increases the surface area available for adsorption of more extracellular matrix protein such as vitronectin and fibronectin [43,45], which further encourage the adhesion of ECs on the surface. The increased ligand density on higher surface roughness sample provided more attachment point for cells. Another randomly roughed (Ti) surface was created by Khang et al. [46] by e-beam vapour deposition to promote endothelialisation. Alteration of deposition parameters produced two surfaces with RMS of 1 nm and 14 nm, respectively. The comparisons of RAEC adhesion on different surfaces were made by a combination of grooved and porous structures, in which a flat valley bottom and a textured peak top were fabricated. To avoid the influence of grooved structure, which will influence the cell attachment behaviour, they manufactured a sample with flat groove top and flat groove bottom surfaces to exclude the influence of grooves and the results showed a non-selective adhesion of RAECs on both top and bottom surfaces. This research reported the potential to promote endothelialisation of the randomly roughened surface. But this setup might not be suitable for attachment comparison because some cells proved to attach to grooves in both ridges and valleys areas. However, the influence of higher roughness, i.e. submicron and micron scale roughness, could differ because the size of ECs is in the micron scale. For instance, research from Xu et al. [47] and Zhou et al. [48] reported two conflicting results on surfaces with roughness in the microscale region: they revealed respectively a lower [47] and higher [48] adhesion of human coronary artery ECs. A possible reason of this could be due to surface morphologies achieved by different manufacturing processes. Surface from Xu et al. [47] was created by electrospinning and the morphology is much different from the randomly roughened surface from blasting, etching and deposition.

SMCs have different responses on surfaces with different roughness. Choudhary et al. [45] prepared different surface roughness on commercially pure Ti and CoCrMo using cold compression metallurgy. Rat aortic smooth muscle cells were utilised for cell adhesion and viability tests. The results showed that the surface with higher roughness had much higher adhesion of SMC, even higher than those on tissue culture polystyrene. However, it was also noticed that the adhesion of SMCs increased more than ECs, and the promotion for both SMCs and ECs is much visible on CoCrMo materials. A systematic analysis of the influence of different surface roughness on ECs and SMCs response was made by Zhou et al. [48]. A gradient surface roughness (Sa) ranging from 0.1 μm to 2.0 μm was created by acid etching on Mg alloy (Fig. 2). Although it was found that, proliferation of ECs was slightly prohibited with anti-corrosion coating in general, it was also found that with anti-corrosion coating ECs exhibited a promoted adhesion and proliferation at roughness between 1 μm and 2 μm, while the proliferation of SMCs was prohibited on all samples especially on surface with roughness above 0.7 μm. This also indicated that the influence of topography is more obvious than the influence of Mg^{2+} concentration. Cell morphology analysis showed that ECs are more flattened and attached firmly on the surface at lower Sa ($\leq$0.7 μm) but tended to attach exclusively onto the top of ridges and have more elongated shape and filopodia at higher Sa ($\geq$1.0 μm). Interestingly SMCs became more elongated, thicker and well-organized at surface roughness below 0.7 μm but become more contractive and smaller on surfaces with Sa $\geq$1.0 μm. It seems that the lower surface roughness in nanoscale could promote both ECs and SMCs growth due to large surface area facilitating protein adsorption, but in surface with micron-scale roughness the promotion is selective for ECs over SMCs. One possible reason could be the change on cell stiffness with varied extent of focal adhesion as shown by the different morphology, considering the different thresholds of directed migration or contact guidance for ECs and SMCs [49]. In this experiment, the roughness threshold for promotion of SMCs proliferation is around 1.0 μm. This threshold could be further explained by the
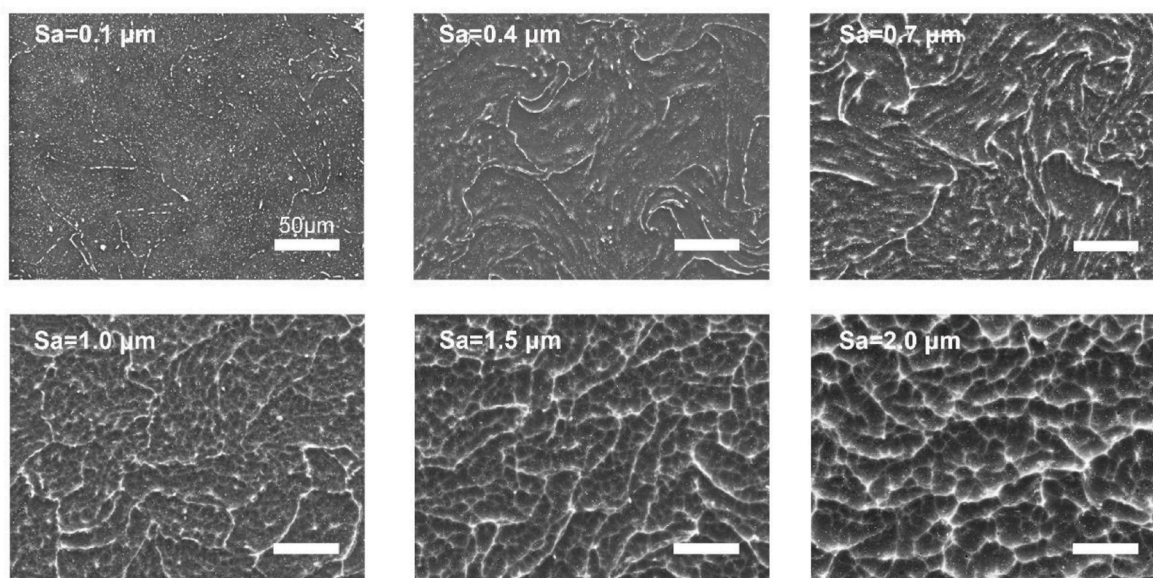

Fig. 2. SEM images of Mg surface with gradient roughness engineered by chemical etching, from Zhou et al. [48]. *Scale bar is* 50 μm.

contact and migration mechanism through filopodia and focal adhesions which act as mechanical sensors during interaction [48]. These sensors on different cells have their own topography preferences and are differ for ECs and SMCs on surface with micron-scale roughness.

Platelet adhesion on randomly roughed surfaces varies according to different roughness and surface wettability. On the one hand, in nano-scale roughness range, it seems that increasing roughness decreases platelet adhesion. Lu et al. [43] fabricated surface roughness (RMS) in the nanoscale region (0.4 nm, 1.15 nm, 14 nm), the 30 min platelet adhesion test showed that the surface with higher roughness has lower platelet adhesion, and platelets density on 14 nm roughness sample is 2–3 times lower than the 0.4 nm sample. On the other hand, in submicron-scale roughness range, the trend is opposite. Linneweber et al. [50] indicated the platelet adhesion increases with increasing surface roughness among three sample with nano to submicron roughness (0.05 μm, 0.20 μm, 40 μm). In these cases, the materials are pure titanium [43] and Ti6Al4V titanium alloys [50], and the results showed that there might be a threshold of roughness in nano scale to obtain low platelet adhesion. There are also other things to be considered for platelet adhesion, such as hydrophilicity and protein adsorption. In both study [43,50], higher protein absorption was found on surface with higher surface roughness, and in research in the nanoscale region [43], there was an increased hydrophilicity with increasing roughness. High hydrophilicity and high protein absorption on the surface are usually considered to be preferable for platelet adhesion [50,51], but a decrease in platelet adhesion has also been reported in another study [43] where the surface with lower hydrophilicity obtained the highest platelet adhesion among three surfaces. Hence, the nanoscale surface roughness and surface hydrophilicity need to be considered together in exploration of their potential for stents application. Collectively, randomly roughened surfaces have demonstrated potential for stents surface texturing by promoting endothelialisation, preventing SMC growth and platelet adhesion. It is worth to investigate further on the threshold promotion of proliferation and platelet adhesion and propose proper surface roughness ranges for stents application.

2.1.2. Grooved structures

Grooved surface structures have also been widely investigated because of their ease of fabrication and their potential to elongate SMCs which have been observed in various previous studies.

Groove structures can promote the proliferation of endothelial cells, and the geometrical dimension of grooves could affect endothelial cells behaviours. Vandrangi et al. [52] produced grating-like grooved sub-micrometric pattern on titanium and silicon surfaces by lithographic patterning, investigating the influence of texture on the growth of human endothelia cells. The grating-like structure is created from a complex process combining plasma deposition, lithographic patterning, Ti deep reactive ion etching (Ti DRIE) and F-based dry etching. Grating structure is grooved-based with 8 different grooves width (0.5 μm, 0.75 μm, 1 μm, 2.5 μm, 5 μm, 10 μm, 25 μm, 50 μm) and fixed groove depth of 1.3 μm, resulting in grating pitch twice the groove width. EC culture results after 5 days clearly indicated that the cell density is highly influenced by the groove width (i.e. ridge width or grating pitch). Lower groove width resulted in higher cell density at 5 days: cell density on 0.5 μm sample is around 3 times of unpatterned sample while cell density on 50 μm sample is similar with unpatterned sample. The sample with lower groove width also resulted in a better EC-related protein expression. This grating-like structure successfully promoted EC adhesion, proliferation, elongation, and orientation. Results from different groove widths also proved the positive effect of ligand density, i.e., groove ridge density in this research, on EC adhesion and growth as ECs are bigger than groove width in this research and are more preferable to attach on groove ridges. However, the increasing ligand density could also cause increasing adhesion of other cells such as SMC and platelets, therefore there should be more investigation on the function of other vessel-related cells to prove the whole effect of this surface structure on

stents. It is also found that the proliferation and migration of ECs are strongly influenced by groove width, depth, and other geometrical dimension of groove textures. Lu et al. [53] investigated the influence of spacing between grooves on the growth of ECs. They utilised lithography patterning and titanium inductively coupled plasma deep etch (TIDE) techniques to create grooves on titanium. TIDE is an efficient plasma dry etching micromachining technique based on anisotropic dry etching of Ti in chlorine/argon plasma. The gentle machining mechanism could pattern surface without debris or damage to minimize the post-processing steps. Quality rectangle and trapezoid grooves were fabricated on the Ti surface with different spacing. Cell culture results clearly showed the strong cell adhesion after 4 h cell culture on nano and sub-micrometre scale surface textures. Cell density characterisation in the following days indicated the negative correlation between cell density and grooves spacing. Cell alignment and density are thus positively correlative with ridge density. Another research reported EC cells aligned within the grooves with 30 μm depth but orientated randomly over the ridges [54]. The possible reason is that the high ridge density provides more cell binding sites and the cells are mainly above ridges (e. g. valleys) because the groove depth created in this study (below 0.5 μm) is lower than ECs thickness. This research provides guidance for promotion of ECs growth, indicating that a nano-scale groove patterning on stents is more likely to promote endothelialisation. However, the influence of groove depth is not investigated and discussed.

Groove structure also has a function to promote the elongation and orientation of smooth muscle cells and fibroblasts. It is also noticeable that the proliferation of SMC is prevented on some groove structures. Another microgroove-structure was fabricated through photolithography-replication methods by Biela et al. [49]. The master silicon was treated by photolithography technique to obtain different groove depths (50, 100 and 200 nm) and groove width (2, 3, 5 and 10 μm). The textured surface was then utilised as a mould to texture the poly (dimethyl siloxane) (PDMS) substrates. Human coronary artery endothelial cells (HCAECs), human coronary artery smooth muscle cells (HCASMCs) and human fibroblast cells (HFCs) were cultured on the textured PDMS surface with different groove depth and width. All three types of cells showed a stronger response on the surface with smaller width and larger groove depth. HFC was more sensitive to surface texture and had a stronger alignment and orientation, but elongation of SMC and EC is not as clear as HFC has a bit elongation and orientation. Additionally, elongation of SMC and EC is also not sensitive of groove depth and width. These results are due to the natural shape and the organisation of cells in tissue. Groove structures have strong influence on the elongation, orientation and migration such as the response of melanocytes on grooved PDMS [55]. The natural shapes of HFC and melanocytes are elongated, thus they are more sensitive to groove morphology. The shape of EC is round and tight cellular junctions are formed as endothelium, hence the guidance of groove structure is not obvious. The response of SMC could not be explained by the shape since the natural shape of SMC is similar to HFC. Consideration of other stimulation is necessary rather than just grooved topographic features are required.

Another grooved PDMS surface by photolithography-replication process was fabricated by Chang et al. [56]. The grooves are 3 μm in width and 5 μm in height. Vascular smooth muscle cells (VSMC) culture results showed the promotion of VSMC elongation and orientation but inhibition of proliferation. Authors revealed that the elongated VSMC were found to be more contractile than synthetic flat shape (Fig. 3). The VSMC on flat surface is more synthetic and epithelial-like, both the morphology, gene expression and biochemical features of flat VSMC are very similar to neointimal cells of the injured artery. This hypothesis from authors explained the reduced proliferation of elongated VSMC, but more importantly it provides another direction for surface engineering of stents, as it is also possible to convert SMC to more contractile phenotype to reduce the proliferation of SMC.

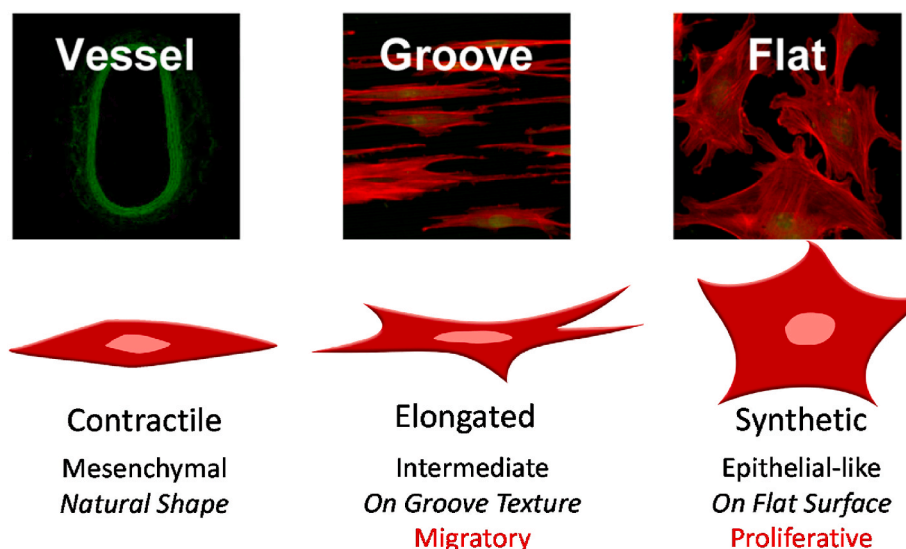Platelet adhesion is also affected by groove surface structure. Ding

Fig. 3. Different shape of smooth muscle cells under different condition, replotted from Chang et al. [56].

et al. [57] investigated the platelet adhesion and activation on groove- and pillar-textured, titanium oxide (TiO_2) coated surface. The ridged width for groove structure is fixed. Two adhesion modes were found for platelet adhesion, bridging and full-contact, on surface with different groove width and pillar interspacing. The thresholds of mode changing for grooves and pillar interspacing are 2 μm and 3 μm respectively, which is similar to the size of platelets. Any interspace above this would lead to platelet attachment on the surface through full-contact mode. Results showed that platelet adhesion on activation via increased bridging was found only on lower groove width and it is higher than those on pillar patterned surface, which has relatively constant platelet adhesion rate at bridging mode. For platelet adhesion at full-contact mode, decreased platelet adhesion and activation were found on surface with larger lower pillar interspace, but for groove texture, increased activation and decreased adhesion were found on surface with larger groove width. The trend for surfaces with pillar textures could be explained that decreased pillar interspace increased contact surface area, but for small pillar interspace, platelet attaches at ridging mode and the change of attach area (i.e. the top surface of pillar) is not obvious when the pillar interspace is changing. This could also be related to the surface hydrophilicity as low hydrophilicity reduced the adhesion of platelets [58] and in this research the water contact angle decreased with decreased pillar interspaces. It is most fascinating to find that the activation and adhesion of platelet on surfaces with 0.5 μm groove width are much higher than other samples: around 50%–100% more than other samples for activation degree and 1 to 2 times more for adhesion rate. This result might relate to the high anisotropy for this sample. 0.5 μm groove width was significantly lower than platelet size (1–2 μm), thus the influence of high anisotropy was evident. High anisotropy could guide cell contacts, this could lead to the activation process of platelet [59], activated platelets then attracts more adhesion of platelets. Another research from Bui et al. [60] investigated the platelet adhesion and activation on grooved surface with 100 nm and 500 nm groove width. Results showed that 100 nm sample got a lower platelet adhesion and activation, which seems to conflict findings from Ding et al. [57]. However, there are several reasons behind this difference. Firstly, the ridged width is the same as the groove width in this research while research of Ding et al. [57] utilised a fixed ridged width when they changed the groove width. Thus, 100 nm samples not only have a decreased groove width, but also increased ligand density. Increasing ligand density could reduce the elongation guidance of groove structure as platelet has more chance to migrate and growth perpendicular to the groove direction. Secondly, 100 nm sample has much lower groove

depth than 500 nm samples, this also reduce the guidance of groove structure. As a results of increase ligand density and decreased groove depth, the platelet adhesion and activation on 100 nm sample is lower than 500 nm sample [60].

Grooved surface could be produced by many techniques, and thus has wide potential for surface modification of stents and related materials. The above studies have proved the efficiency of grooved surface structure, but the influence of groove dimension, such as relationship between the promoted proliferation of ECs, platelet activation and groove dimension, have not been systematically analysed. The possibility to improve endothelialisation and selectively prevention of SMCs growth as well as to combine with surface chemistry modification also need more investigation.

2.1.3. Tubular and pillar structures

Nanotubular surfaces could potentially induce quick endothelialisation. Sharp and dense nanotubular surface structures were produced on a CoCr alloy, MP35 N by Loya et al. [61] through RF plasma. The nanopillars have high aspect ratio (>10:1), with an average height of 3 μm and average diameter of 220 nm (Fig. 4). Although the surface chemistry did not exhibit obvious changes after RF plasma treatment, the hydrophilicity dramatically increased. Bovine aortic endothelial cells (BAEC) cultured on the nanopillar surfaces revealed low oxidative stress and presence of peri-junctional cortical band of filamentous actin, while the untreated surface has relatively higher oxidative stress and absence of filamentous actin between cells, proving the increased biocompatibility of the textured surface. This sharp, dense nanotubular surface structure provides a lot of attachment points for BAECs as the nanotubular structures also increase surface area for cell attachment, thus increasing the proliferation and migration of BAECs. Hence, this nanotubular surface structures could potentially encourage endothelialisation. Still, effect on VSMCs and platelets should also be investigated to provide a complete view of the function of this type of structures. There is another evidence for fast endothelialisation of nanopillar structures from Csaderova et al. [62], who textured polycaprolactone (PCL) through duplication method. Silicon wafers masters were fabricated by electron beam lithography, and nanopillars on PCL was hot embossed by melt moulding and hot pressed. The size of nanopillars was around 100 nm in diameter, 115 nm in height and a pitch of 300 nm. Human fibroblasts (hTERT) and endothelial cells (b.End3) were cultured on both flat surface and the surface with nanopillars. Results showed clearly that hTERT cells grew slower but b.End3 cells grew faster on the surface with nanopillar after 96 h. To exclude the influence of air
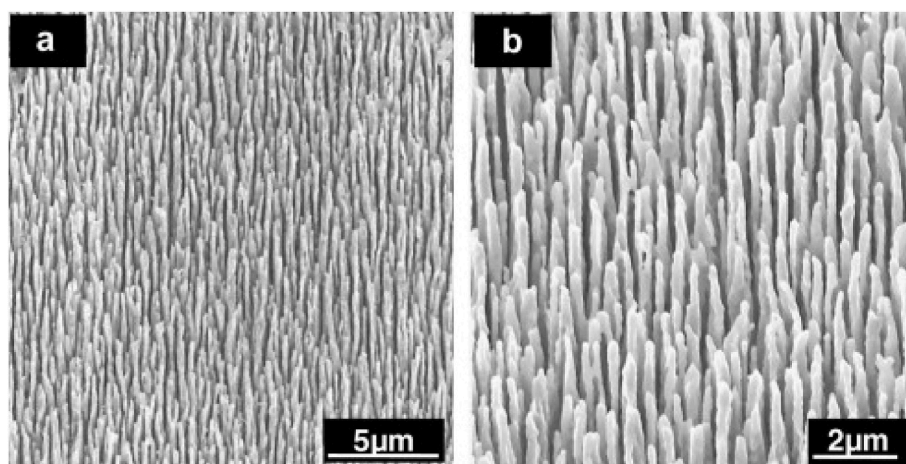
Fig. 4. Nanopillar surface structure on CoCr made through RF plasma from Loya et al. [61] *at (a) low magnification (b) high magnification.*

bubbles captured by nanostructure on the cell growth, different coatings were used but same results were observed. It is indicated by researchers that the prevention of fibroblast cells is due to the inadequate ligand density on the treated surface, but the reason for the promoted endothelial cell growth was not provided. The possible reason could still be related to the ligand density and natural cell shape of ECs. The hTERT cells on the flat surface is more extended with size around 200 μm in length and 50 μm in width, while the b.End3 cells on nanopillar surface is more round with size around 100 μm in diameter. It is anticipated that the lack of guidance on migration due to absence of pattern surface restricted the elongation of fibroblast cells, but the multidirectional lattice of micropillars still can support the proliferation and migration of round endothelial cells. Overall, nanopillar or nanotubular structures could promote increased endothelial cell growth, even when different shapes and sizes are considered.

Nanotubular surface structures could also prevent the proliferation of SMCs. Lee et al. [63] utilised anodization method to produce nanotubular structures on nitinol foils. The nanotubes were around 100 nm in diameter and mainly formed by NiO and TiO$_2$. The selected topography resulted in a promotion of the growth and elongation of human aortic endothelial cells (HAEC) and the prevention of the proliferation of human aortic smooth muscle cells (HASMC). It is indicated that this surface has a high potential to promote the endothelialisation and prevent the neointima.

The function of nanotubular surface structure on platelet adhesion is related to the pillar interspace and pillar top surface. Milner et al. [64] fabricated nanopillar on polyether (urethane urea) (PUU) by lithography two-stage replication moulding. Two interspaces with the same dimension of the pillar diameter were utilised for texturing of surface

with 400 nm and 700 nm nanotubular, while the depth for these two textures was kept similar. The platelet adhesion test was processed at different sheer forces in phosphate-buffered saline. All samples present a low platelet adhesion at high sheer force, but at lower sheer force, the sample with 400 nm depth showed the lowest adhesion, and the untreated surface showed the highest adhesion. This may relate to the small attachment area available as the platelets are all observed adherent to the top of the pillars. Another research from Ding et al. [57] derived similar results when platelets attached on the top surface (Fig. 5). There is a threshold around 2–3 μm for pillar interspace (with dimensions as the pillar diameter) between bridging adhesion and full-contact adhesion. At low pillar interspace range (i.e. bridging adhesion mode) platelets adhesion rate decreased with the decreased interspace. At full-contact mode, adhesion rate decreased with increased interspace. This might also relate to the reduced attachment area: the attachment area reduced with decreasing of pillar interspace at bridging mode due to the reduced top surface area but increased with decreasing of pillar interspace at full-contact mode due to the increasing of surface area. It is noticed that almost all samples except the 16 μm samples showed higher adhesion rate compared with flat sample. The reason was not explained but could be that the radio frequency (RF) sputtering deposited TiO$_2$ surface could has small roughness [65] which might reduce the adhesion of platelets. In summary, the nanopillar surface can be designed to control platelet adhesion, indicating the possibility of application for stent surface topography.

The selective promotion of endothelialisation over prevention of SMC growth and reduced platelet adhesion at selected pillar interspace and diameter are two impressive achievements of nanopillar or nanotubular surface structures. Still, it is not easy to fabricate this texture
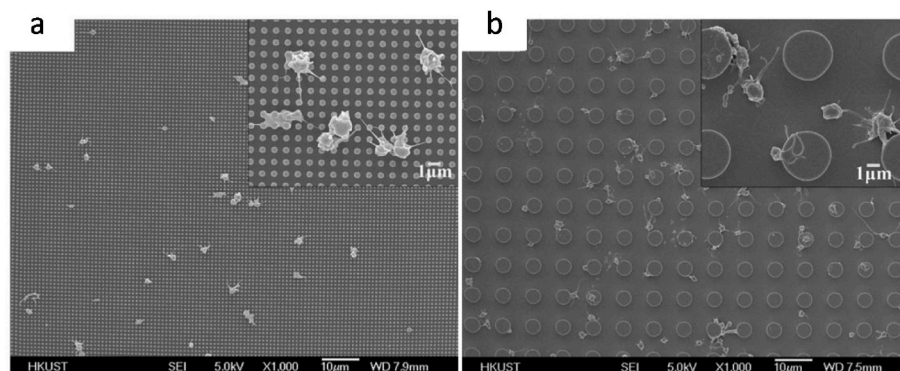

Fig. 5. Platelet adhesion results showed the different attachment mode and different activation condition: (a) Bridging mode of platelet, pillar interspace and diameter are 0.5 μm; (b) Full-contact mode of platelet, pillar interspace and diameter are 4 μm. From Ding et al. [57].

with desired chemistry on stents because nanopillar fabrication process is usually accompanied by unavoidable chemistry modification. Expanding the possible fabrication methods on polymeric materials is also essential as the lithography two-stage replication moulding is not well suited for the fabrication process of stents.

2.1.4. Porous structures

Porous or crater-like surface structures are another type of geometry utilised in biomedical devices, especially for orthopaedic applications. However, the pits or porous structures can potentially be applied on stents too.

Some studies reported on the effect of porous surfaces on endothelial cells, but negligible promotion was reported. Macro (pore diameter of 1–1.5 μm) and nano (pore diameter <15 nm) porous surfaces were made on silicon by Formentín et al. [66] through etching. Human aortic endothelial cells were subsequently cultured to check the cell viability. Both macro and nano porous surfaces hindered the growth of ECs after 9 days. The cell exhibited round shape on nano porous surfaces indicating the poor attachment of cells. Similar results were also reported by Casillo et al. [67]. They investigated the attachment and growth of human umbilical vein endothelial cells on porous silicon with 3 and 0.5 μm pore sizes. Porous surfaces with smaller pore size resulted in fewer focal adhesion and shorter fibronectin fibrils after 24 h, indicating the poor adhesion of ECs on the surface.

Porous surface structures have the potential to affect platelet adhesion. Two porous alumina membranes surfaces with 20 nm and 200 nm pore size were used for whole blood contact tests [69]. The results showed that platelets on 20 nm sample have been activated, but platelets were hardly seen on 200 nm sample (Fig. 6). This study indicated the importance of texture size for platelet adhesion and activation.

Porous surfaces are not normally favourable for stents because the environment in which they operate is not porous, and the flowability of blood on the porous surface will be influenced as porous surface has large areas to trap blood. But porous structures still have the potential to reduce platelet adhesion and activation. The function is also related to the size of features and cooperation of blood cells and protein adsorption. Thus, it is worth exploring further on the influence of porous or crater-like texture on stent performance. Although porous surface was indicated to be not sufficient to promote endothelialisation, it could still offer potential applications for polymer-free drug-eluting stent surfaces.

The porous surface could act as drug-carrier, but the quick releasing of drug is another problem which needs to be considered [68].

2.1.5. Wired and spaghetti-like structure

Nanowires and spaghetti-like structures have attracted some interest in recent years, as they are very different comparing to regular surface structures. Their fabrication methods are relatively complex, but nanowire structures proved good performance for their application on stents.

A nanowire structure shown in Fig. 7a was created on aluminium oxide through chemical vapour deposition (CVD) by Aktas et al. [71]. Two different nanowire densities, low density (LD) and high density (HD) were fabricated on the aluminium oxide and then human umbilical vein endothelial cells (HUVEC) and human umbilical vein smooth muscle cells (HUVSMC) were cultured on the textured surfaces. The results indicated that the attachment on the textured surface of both HUVEC and HUVSMC decreased compared with normal aluminium oxide. HUVECs had a delayed proliferation on the HD nanowired surface and both HUVEC and HUVSMC has an abnormal morphology on HD surface. Further cell morphology analysis proved that the HD surface is not suitable for cell attachment and proliferation. On the other hand, although the attachment and proliferation of HUVECs is still not as good as on non-treated surface and smooth glass surfaces, the LD surface selectively promoted the attachment and proliferation of HUVECs. In total, this nanowire surface has potential to selectively promote endothelialisation instead of the growth of SMCs, but there is still a poor attachment and proliferation of ECs on the surface compared with non-treated surfaces. Another method to fabricate nanowires structures on stents (Fig. 7b) was proposed by Mohan et al. [72], who claimed the selective promotion of the proliferation of HUVECs and less in-stents restenosis. The nanowire surface structures were fabricated by thermal hydrolysis of Ti coatings which is sputter coated (also known as CVD) on stainless steel. This surface is super hydrophilic and the 72 h proliferation after cell culture shows that ECs grew much better on textured surface than bare surface although the initial adhesion on textured surface is weak. Another interesting finding is that the proliferation of SMCs was obviously inhibited on textured surfaces compared with bare surface. Further *in vivo* implantation in rabbit iliac arteries shows the reduced neointimal hyperplasia of textured stents than bare stents. Additionally, the textured stents clearly showed the well coverage of ECs, indicating the quick endothelialisation. Suitable mechanical
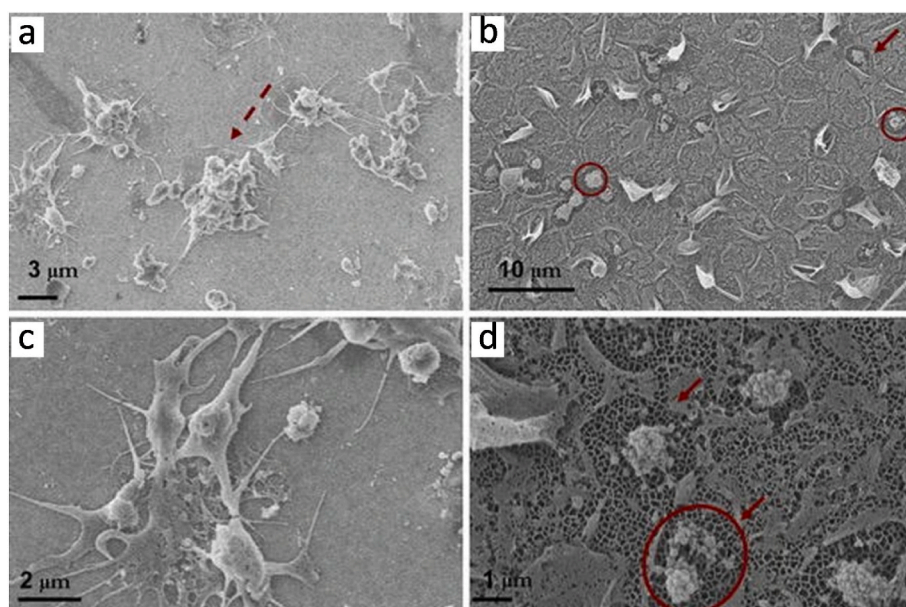

Fig. 6. SEM images: (a, c) 20 nm porous alumina surface; (b, d) 200 nm porous alumina surface after whole blood contact test, from Ferraz et al. [69]. *The arrows and circles indicate the platelets.*
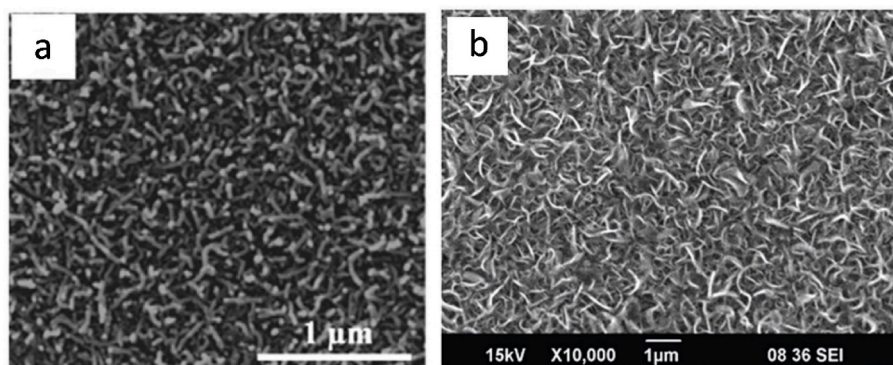
Fig. 7. Nanowire structures fabricated by CVD from (a) Aktas et al. [71] *(b) Mohan* et al. [73].

properties such as crack resistance and radial stiffness were also indicated in another research [73]. Hence, the nanowire surface structures showed significant selective promotion of endothelialisation and may be applied to modify stent surface and reduce in-stents restenosis. The selective promotion of endothelisation could be due to the surface morphology. The nanowire structures provide plenty attach points of HUVECs, but the isotropic morphology prevents the elongation of SMCs because of the lack of guidance from surface structures. However, because the surface structure is created by thermal hydrolysis in NaOH, the contribution of surface structure to endothelialisation would be clearer if information on surface chemistry would have also been included.

The nanowire structure exhibits good performance showing potential to selectively promote ECs growth while prevent the growth of SMCs, which is essential for stents. One problem is that this structure is mainly produced by vapour deposition and hardly fabricated by other techniques. There should be further investigation on the production of nanowires by other surface modification techniques.

2.1.6. Combined and hierarchical structure

The combination of different textures could induce a more efficient improvement in stents performance, even better than single surface structures, as it could make hierarchical structures available on defined areas.

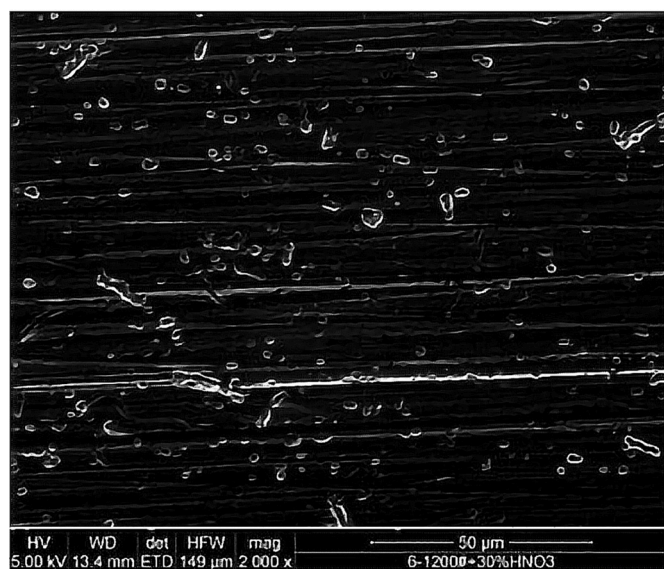Micropores and microgrooves on biomedical nitinol alloy (NiTi)

Fig. 8. SEM image of hierarchical surface texture with pores and grooves fabricated from chemical pickling and grinding, from Shen et al. [74].

were created through grinding, chemical pickling, plasma nanocoating and their combination by Shen et al. [74] as shown in Fig. 8. The original surface was firstly polished, followed by different surface treatment to obtain different geometries, including grinding for microgrooves, chemical pickling for micropores, grounding with chemical pickling for microgrooves with micropores. The micropores were all randomly distributed on the surface and microgrooves were unidirectional, the distance between two grooves was approximately 2.5 μm and the distance between two pores was 3 μm. The size of the pores and grooves respectively was around 1 μm and 0.5 μm. Plasma processing was used to deposit SiO_x:H on the surface. As characterised, plasma flattened the polished surface, and did not change the morphology of other treated surfaces. The results showed that the microgroove-micropores topography had highest ECs cells adhesion, and the SiOx:H plasma nanocoating significantly increased ECs proliferation and adhesion performance. According to the size of the microgrooves and micropores, the micro-size topography played a role to induce cell orientation and cell proliferation. The influence of certain element on the surface to the cellular response is not clear because the plasma coated Si, C and O on the surface together. However, some studies proved that the carbon coating on the surface did not make a significant difference [75], while some researchers proved the positive effect of oxygen on endothelialisation [76]. Thus, this combination of microgrooves and micropores was proved to be a potential method to improve performance of stents, although it would also require further consideration on the possibility of simultaneous surface chemistry modification.

Kiefer et al. [77] creatively combined CVD and laser surface treatment to produce a novel nanowire/micropits aluminium–aluminium oxide (Al/Al_2O_3) multi-phase surface topography on the biocompatible glass as shown in Fig. 9. CVD was firstly used to produce the spaghetti-like nanowire structures on the surface and then Nd:YAG laser was used to generate spot arrays on the nanowire structure. These were 45–50 μm in diameter, 100 nm in depth and 150 μm in interspacing. The secondary random porous structure was produced by laser within the micro-pits because of the rapid heating and cooling. HUVEC and HUVSMC were cultured on the treated surfaces. Compared with HUVSMC, HUVEC had better attachment and proliferation on both nanowire structure and multi-phase structure. The proliferation of HUVSMC was greatly hindered on both treated surfaces. However, both HUVEC and HUVSMC showed a lower activity and slower growth on the treated surface than control bare glasses. This research indicated the selective prevention of HUVSMC on both nanowire and nanowire/micropits structures, but the decreased activity and growth rate of HUVEC should also be addressed in any future study.

The study of combination of different textures still needs more investigations as the combined texture is not always efficient for the functionality designed. However, combination of various type and shapes of texture across micro and nano scales might have different and more interesting function, which needs more novel design and careful
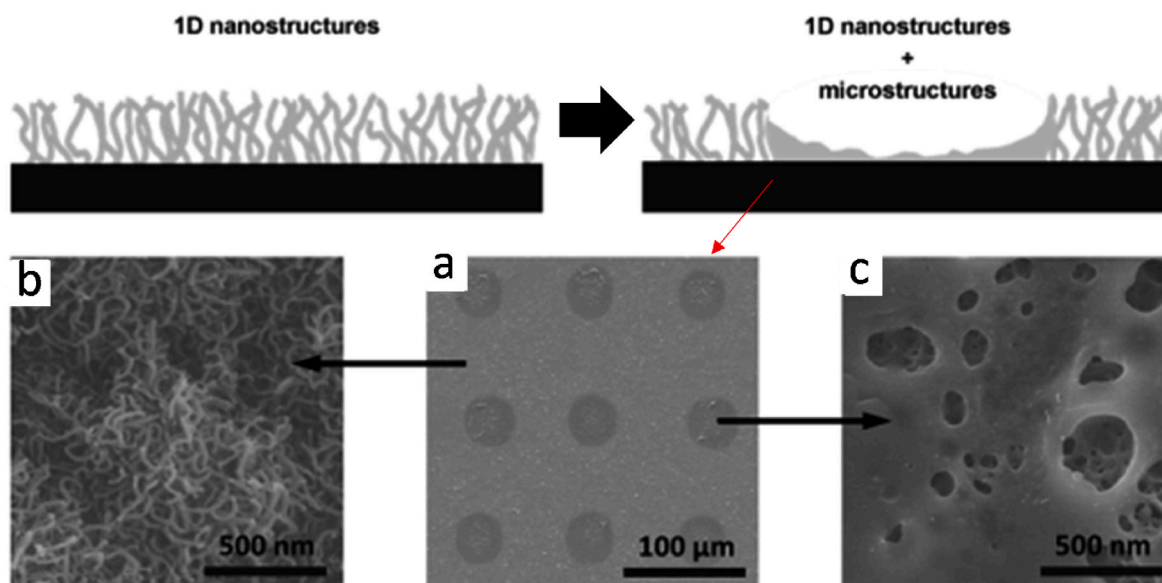
Fig. 9. Schematic pictures of nanowire/nanopits hierarchical texture fabricated by CVD with laser ablation [77]: *(a) SEM of the nanowire/nanopit texture; (b)SEM images of nanowire texture; (c) SEM images of pores inside nanopits.*

consideration.

2.1.7. Summary of topographical effects

Surface topography affects many surface properties such as wettability, protein adsorption, ligand density and shape. The complex and combined effects of these properties could significantly influence the biological response of textured surfaces. The feature size and interspace between features have great influence on the attachment mode of cells. Because cells favour attachment to larger areas with adequate ligands, they intend to attach and growth into the interspaces (deep) or on the top of features (valleys) when these are much larger than the cell size. For example, platelets are found attached at the interspaces between groove ridges and pillars [57]. For many features ranging from nano to submicron domain, cells bridge between features and these features act as ligands for cell attachments, proliferation, and migration. Behaviours are then strongly affected by ligand density and features orientation. Round, relative flatten, fine and large amount of ligand usually provide a high potential for improvement of endothelial cells which is around 50–70 μm long, 10–30 μm wide and 0.1–10 μm thick [78], such as randomly roughened surfaces with roughness ranging in the nano to submicron scale [43,44,46,48], nano pillar surfaces [61,62] and nanowire surfaces [71,72]. If the features have preferential orientation or the arrangement of features is anisotropic, features then provide an oriented guidance for cell growth and migration, as demonstrated by the strong alignment of smooth muscle cells on groove structures [49]. This guidance will induce some change of cells shape and function, especially for smooth muscle cells [56] which help in the reduction of proliferation of smooth muscle cells.

Topography also strongly influence the wettability of the textured surfaces [79] and surface protein adsorption [44,50]. The influence of wettability is complex. High wettability increases the attachment area between liquid environment and surface, thus increasing the interaction between biological environment and biomedical devices. This influence should be universal for cells but surface with lower wettability could be both preferable for platelet adhesion [44] and unpreferable for endothelial cells [43]. The influence of topography and surface chemistry still dominate the cells response. A higher protein adsorption could result in higher cells attachment, and this is universal for both platelets adhesion [50], endothelial cells [43] and smooth muscle cells [80]. Hence it is good to test the wettability and protein adsorption, but topography modification is still more important.

Almost every surface structure has a positive function for promotion of ECs growth, but the prevention of SMCs growth and platelet adhesion are not clear for some surface structures as shown in Table 1. It is also vital to consider the influence of geometrical dimension of texture and distance between textures and influence of surface chemistry. The potential improvement of rapid endothelialisation and prevention of SMC proliferation caused by combined texture on stents should also be carefully considered. For laser surface texturing, grooves and craters are more easily to fabricate, but with the help of nano-texturing technics such as laser-induced periodic surface structure, it is also possible to fabricate randomly roughed structures nanotubular structures and nanowires. The understanding of influence of topographic features on cellular response of blood vessels would help to guide the direction of laser texturing for stent surface engineering.

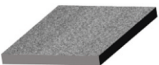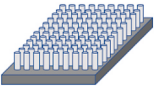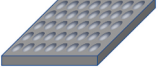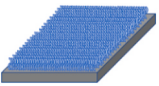*2.2. Influence of surface chemistry on stents performance*

Surface chemistry is another essential aspect to consider for cell-surface interaction. Although surface chemistry modification is usually accompanied with topographical changes, surface chemistry modification still deserves more investigation for improvement of ECs growth, prevention of SMCs growth and low adhesion of platelets. Coating is a popular method for surface chemistry modification and other surface functionalities such as oxidation and nitridation which are also important for stents.

2.2.1. Coatings

From inorganic to organic materials have been coated on stents surface, even some natural biological coatings were investigated, but not all the coatings provided an improved performance for stents. Plenty of inorganic coatings are available for stents surface modification, including diamond-like carbon, nitrides, oxides, silicon carbide and hydroxyapatite-based materials.

The positive function of several inorganic coatings has been proved. Titanium-nitride-oxide (TiNOX) proved to be an efficient coating material for stents. As the titanium oxide (TiO_2) is already a good coating for biodevices with a high request for hemocompatibility [81], TiNOX coatings has even lower platelets adhesion and fibrinogen adsorption than TiO_2. Animal tests proved that TiNOX coatings reduce neointimal hyperplasia [82], and a large amount of clinical data also proved that the TiNOX coated stents show a good clinical performance [83–85], but

Table 1
Summary of different surface texture.

Texture	Illustration	EC	SMC	Platelet	Other
Randomly Roughened		• Improved adhesion in nano to submicron roughness range [43,44, 46,48]	• Prevention in nano to submicron roughness range [45,48,49]	• Reduced adhesion at around 15 nm roughness range [43,50]	• Influence is highly roughness-dependent [43–46,48,50]
Grooved		• Improved adhesion and proliferation of EC [53] • Alignment [53,54]	• Reduced proliferation [56] • Alignment in the groove direction [49,55,56]	• Reduced platelet adhesion at submicron groove size and interspace [57,60]	• Ridge density↑=> Cell alignment↑ Cell density↑ [57]
Nanotubular		• Improved adhesion and proliferation of EC [61, 62]	• Prevention of proliferation and migration of SMCs [63]	• Reduced platelet adhesion at around 500 nm nanopillar size and interspace [57,64]	• Influence is highly pillar size and interspace dependent [57]
Porous		• Reduced adhesion and proliferation of EC [66, 67]	• No research data, but the trend could also be highly feature-size-related	• Reduced platelet adhesion at 200 nm hundreds nanometres pore/crater size [69,70]	• Conflict performance test [66,67,69,70] • Drug carrier ability [68]
Nanowire		• Improved adhesion and proliferation of EC [71, 72]	• Prevention of proliferation and migration [71,72]	• No research data, but nanowire surface might get reduced platelets adhesion according to results from nanotubular structure	• Mainly produced by vapour deposition [40, 71,72]
Combined	Combined Surface Texture	• Potential to promote ECs growth [74,77]	• Potential to prevent SMCs growth [77]	• Potential to reduce platelet adhesion with some former stated structure and feature sizes	• Performance should be further investigated

there are also come clinical results showing that the DES with novel drugs has better clinical performance than TiNOX coatings [86]. Thus, TiNOX coatings still need an in-depth investigation to be competitive within the development of DES. It is also possible to combine the TiNOX and drug carrier to fabricate novel stents.

Carbon and silicon carbide coatings are also widely used for stents. Previous research proved that diamond-like carbon coatings could reduce platelet activation and Ni, Cr metal ions releasing [34]. A better clinical performance for pyrolytic carbon coatings (Carbofilm™) has also been demonstrated [87–89]. But carbon coatings are relatively stiff for stents as stents are usually balloon expanded, thus clinical results showed a reduced performance of stents when using carbon-based coatings [90]. Carbon coatings still need more investigation, for example the semiconductor coatings with doping silicon [91]. Due to the semi-conductivity ability silicon related materials (for example silicon carbide, SiC) are also potential candidates for stents coatings. But the performance of SiC is somewhat contradictory: although SiC proved to be low platelet adhesive [92] and has lower Ni ions releasing [93], their clinical performance is not obviously increased in all cases [35]. Overall performance of inorganic coatings is not fully convincing, but their semiconducting potential could reduce platelet coagulations. Additionally, inorganic coatings are also usually applied by laser, which need further investigations.

Biocompatible polymeric coatings are also important coatings for stents. In the early stage, some polymer coatings aim to provide a more hemocompatible surface of BMS [94]. But polymers are mainly applied as drug carriers and corrosion control layers. As drug carriers, organic coatings are classified into durable coatings, such as poly (styr-ene-b-isobutylene-b-styrene) (SIBS) [95], polyethylene-co-vinyl acetate (PEVA) and poly (n-butyl methacrylate) (PBMA) [96]. The performance of durable polymer coated stents is usually better than BMS during the first year of implantation [95], but it usually causes long-term problems such as very-late thrombus [96] due to the lack of biocompatibility of durable polymers. Hence, biodegradable polymers have been applied as stents coatings. Poly-l-lactic acid (PLLA) and poly (lactic-co-glycolic acid) (PLGA) are two popular coatings materials and there are already many commercial DES with these two drug carriers such as PLLA coated Nobori® stent [97], Excel® stent [98] and Cura™ stent [99], and PLGA coated stent Infinnium™ stent [100] and Sparrow™ stent [101,102]. Bio-originated and biomimetic polymer coatings are other two types of novel and popular coatings for stent applications. Some of these coatings have good performance as stent coatings, such as phospholipid-based

coatings [103], phosphorylcholine-based copolymers [104] and mussel-inspired hydrogel [36]. The high biocompatibility and hemo-compatibility of these coatings are important properties. Organic coatings also include natural biological coatings. These coatings are formed of all-natural components found in the body; hence they are all highly biocompatible. Fibronectin and type I collagen could enhance cell attachments, but this enhancements is not universal for both ECs [105, 106,106,107] and SMCs [80,108]. Heparin has the ability for anti-coagulations [109], but also could promote proliferation of ECs [110] and prevention of SMCs growth [111]. While albumin could prevent the adhesion of cells [112,113] and thrombus formations [114]. Natural biological components are not commonly used as coatings because they are usually absorbed soon after implantation of stents, furthermore the coating processes for these components is complex (e.g. layer-by-layer deposition [115,116], covalent bonding [117] such as GORE® TIGRIS® vascular stent [118]). Overall, organic coatings are vital for stent applications. Laser coating of these materials and components is relatively difficult, but laser could increase the bonding between these components and stents because the durability of the coating is also important for long-term performance of stents.

The function of coatings is highly materials-dependent and the durability and ion-infiltration need to be carefully investigated because they are vital for the long-term performance [9,36,119].

2.2.2. Other surface functionality

Other functionalisation techniques via modification of surface chemistry to improve the performance of stents include surface nitridation, oxidation, electrochemistry modification in addition to simple coating methods. Some of the techniques can still be considered as coatings methods but are able to produce more multi-functional coatings by complex steps and some combination of several modification technics were also possible for stent surface functionality.

The positive influence of nitridated stent surface was found in several investigations. Except the titanium-nitride-oxide coating, normal nitridated surface is also efficient, such as the 316L stainless steel surface textured in nitrogen by laser by Li et al. [120]. Several nitridated metal components was found on the laser treated surface, including nitridated Fe and Cr, this surface showed a unique promotion of endothelialisation compared with the surface treated in air and argon [120]. Another nitridated 316L stainless steel surface was created by low-temperature plasma nitriding by Braz et al. [121]. Although their conclusion was derived without the consideration of roughness, they also claimed an

increased viability of ECs on the treated surface. The mechanical properties are also improved by surface nitridation. It is indicated that the nitridation of NiTi surface by both plasma nitridation in nitrogen [122] and plasma immersion ion implantation [123], increasing corrosion resistance, surface hardness and modulus. There is also a research investigated the platelet adhesion on nitridated Ti alloy and indicated the low platelet adhesion on the nitridated Ti alloy [124]. It is possible to conclude that the nitrogen element on the surface is a preferred for attachment, growth, and migration of ECs and has potential to prevent platelet adhesion.

Another important direction for stents surface treatment is the formation of nitrogen oxide (NO). NO is a crucial modulator influencing the reconstruction of target vessels. It could prevent the adherence of platelets, proliferation and migration of SMC, chemotaxis and migration of leukocyte, as well as promote endothelialisation, and relaxation of vascular [125]. NO releasing surface is mainly achieved by coatings. NO generating materials could be divided into N-diazeniumdiolated based NO release polymers, Nitrosothiol-based NO release polymers and catalysed materials for endogenous NO generating [126]. Endogenous NO generating is more durable than other NO donor coatings, such as a 3, 3-diselenodipropionic acid (SeDPA) with glutathione peroxidase (GPx)-like catalytic layers fabricated by Yang et al. [127], there are also other investigation trying to achieve the non-coating method for NO generating. For example, McCarthy et al. [128] investigated the catalytical ability of different metal ionic for endogenous release of NO from S-Nitroso-N-acetyl-d-penicillamine (SNAP). The results showed the endogenous NO generating ability of Co^{2+}, Ni^{2+} and Zn^{2+} at physiological conditions and this could be applied in the design of biodegradable stents. NO generating surface is attracting a lot of attention for stents surface treatment. It has huge potential to be one of the feasible research directions for surface modification and functionalisation of stents.

Oxidation is an achievable surface functionality for stents, but the biological improvement for stents application is limited compared with nitridation. The oxidation treatment is usually for the improvement of electrochemical properties rather than biological properties. For example, Li et al. [120] claimed that the laser treated stents in air failed to improve the EC proliferation. While the Ti–O layer on 316L [129] and oxidation layer on NiTi [130] improved the corrosion resistance and thus reduced the hazardous metallic ions releasing. There are also some novel oxidation treatments of stent surface which increased the endothelialisation. Kakinoki et al. [131] immobilized a EC adhesive peptide on 316L and CoCr stent surface by single-step tyrosine oxidation with copper chloride (II) and hydrogen peroxide. The results showed an increased HUVEC adhesion and decreased platelet adhesion. The improvement was promising, but the achievement of improvement is mainly due to the EC adhesive peptide. Another important aspect is the control of the stent degradation. A comparison was made between magnesium biliary stent with and without micro-arc oxidation [132]. The treated stents showed an obviously slow degradation compared with stent without oxidation in human bile in vitro. The influence of oxidation on stents application is mainly concentrate on the mechanical properties, such as increasing corrosion resistance and control of degradation, it also usually reduced ions releasing to influence biological response indirectly.

Nitridation and NO releasing surfaces are two possible research directions for surface treatment of stents, while oxidation could also be used as a pre-treatment method. The influence of nitrogen element to biological response is still not fully investigated, but the ability to promote endothelialisation is vital for stents.

2.2.3. Summary of effects of surface chemistry

Surface chemistry is another vital aspect to consider in surface engineering of stents. Different surface chemistries result in different surface wettability [79] and protein adsorption. Additionally, cells have preferential surface chemistries for attachments. Surface modification

methods can be divided into coatings and surface functionality. Coating is a straight-forward modification of surface, but the addition of layers of similar/dissimilar materials. Sometimes coating is not efficient as it can delaminate from the substrate, especially for organic coatings. But coatings with nitrogen, bio-originated organic coatings and coatings of natural biological drugs or materials have positive effects on stents performance.

Another interesting surface chemistry modification is surface nitridation, which proved selective promotion of ECs over SMCs and reduced platelets. Laser has the ability for coatings and surface functionality, and these findings provided several directions for laser surface modification of stent surface, such as laser surface nitridation. Combined with texturing, laser could fabricate a surface with both suitable texturing and desired surface chemistry.

3. Laser surface modification on stents and stent-related materials

Laser surface engineering has several advantages among other surface modification methods, being precise, selective, and ultra-fast as well as providing access to various geometrical designs. Laser surface engineering is much suitable for the modification of stents because of the small size of stents and the requirement of precise, tailorable, and clean modification. Several groups of researchers have investigated Laser surface engineering on stents or stents-related materials achieving different textures and surface chemistries and testing the resulting performance of stents in vitro and/or *in vivo*.

3.1. Laser surface texturing on stents and stent-related materials

Laser texturing is a suitable technique to manufacture grooves, pits, pillars, and complex freeform surface structures. These surface textures (Table 1) enable changes to functional properties of stents.

3.1.1. Direct laser patterning

Grooved surface structures are still popular for laser surface modification of stents because of their ease of fabrication. One method to fabricate grooved structure is via laser ablation. Li et al. [120] fabricated groove-like structures by laser ablation on 316L stents. According to their analysis, it is possible to fabricate a biomimetic grooved structure similar to the luminal surface of rat aorta as shown in Fig. 10 using optimised laser parameters. After the culture of endothelia cells, a threefold increasing of cell adhesion and eightfold for proliferation is found. However, it is very interesting that the increasing is only obtained in nitrogen environment compared with the laser processing in argon. Further experiments should aim at comparing other surface structures with different surface chemistry conditions and associate performances.

A spots array surface structure was generated by Oberringer et al. [133] on 316LS stainless steel by Ti:Sapphire femtosecond laser. The size of spots is around 50 μm, with tracking distances being 75 μm (high density, HD), 125 μm (MD) and 175 μm (LD). Co-culture of normal human dermal fibroblasts (NHDF) and human dermal microvascular endothelial cells (HDMEC) results showed clearly decreasing proliferation capacity of MF on both HD, MD and LD surface, while a slightly decreased cell density of HDMEC compared with controlled non-treated on LD and MD surface. Additionally, HD surface showed a relatively poor cell proliferation of HDMEC. However, since the HD surface has the lowest wetting angle, highest roughness, and oxygen content among three surface structure design, it is hard to conclude the relationship between the proliferation of co-culture cells and textured surface [134]. The reason of failure in promotion of proliferation of ECs might be the large size of spots (around 50 μm) and the large interspace (75 μm–175 μm) between lines. Both laser spot size and line interspace are similar to the size of ECs [78], thus the features is too large to provide enough ligands for ECs. It is worth reducing the texture size to check the cell response.
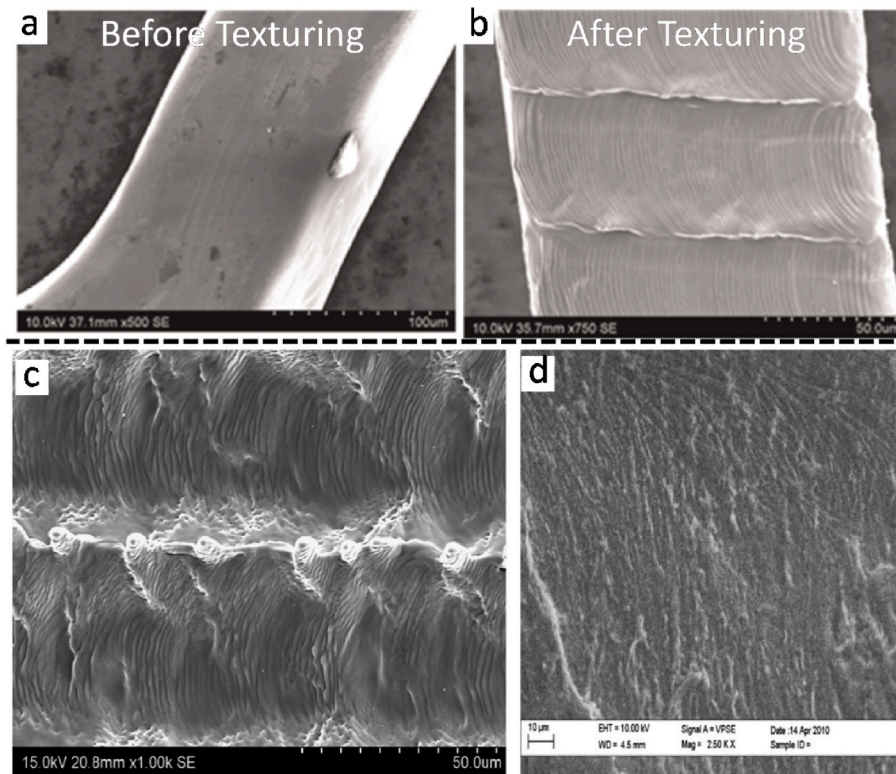
Fig. 10. Comparison of original stents surface, laser ablated surface and luminal surface of rat aorta. (a) untextured stents surface (b) textured stents surface (c) biomimetic grooved surface on 316L in nitrogen made by Li et al. [120]*; (d) the inner luminal surface of rat aorta.*

Another method to fabricate grooved structure on surface is direct laser interference patterning (DLIP). DLIP technique use beam splitters to create two or more laser beams, these beams then interfere and fabricate various regular patterns including grating-like grooves on the surface. Grooves with more controllable depth, width and periodicity could be created by DLIP. Schieber et al. [134] fabricated grooved

surfaces structure on CoCr alloys by DLIP technique. Several laser incident angles and fluencies have been operated and created several groove patterns with different periodicities (valley to valley distance, 3 μm, 10 μm, 20 μm, 32 μm) and different depth (<40 nm and >600 nm). SEM pictures in Fig. 11 show that the grooves are clear and neat. Further platelet adhesion tests show the reduced adhesion of platelets for all
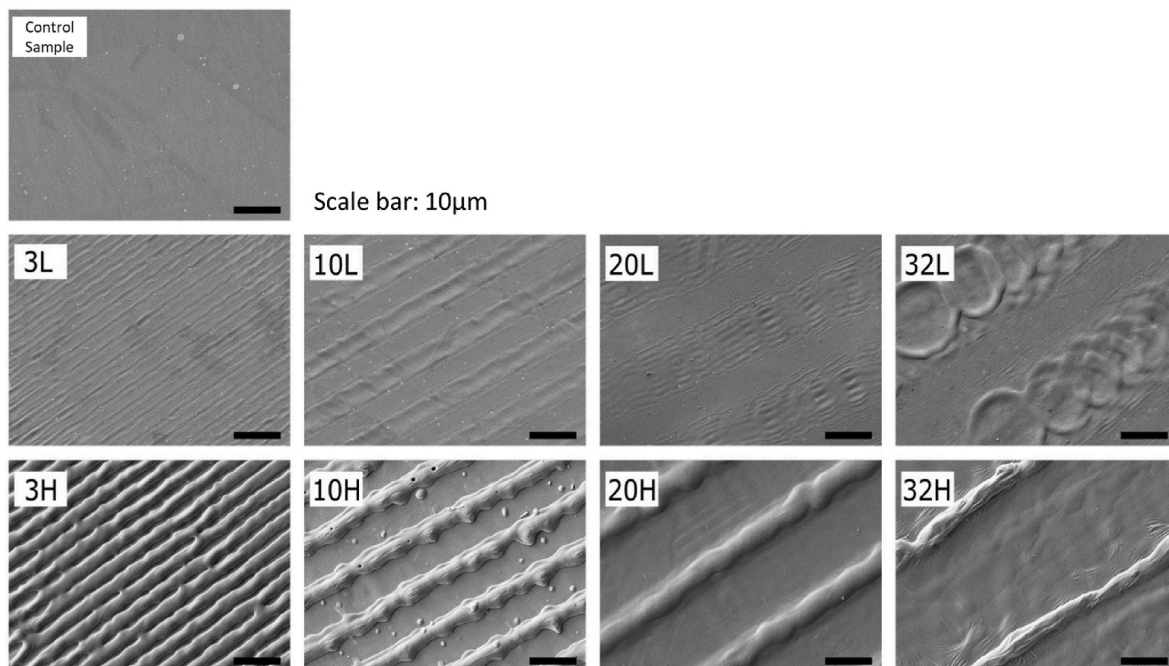

Fig. 11. SEM images of plain CoCr and DLIP textured samples fabricated by Schieber et al. [134] *with different periodicities (valley to valley distance,* 3 μm, 10 μm, 20 μm, 32 μm*) and depth (*<40 nm, L; >600 nm, H).

laser treated samples, especially 32L and 32H, but the HUVECs culture results only shows the elongation of ECs on H samples, while the cell density on all laser treated samples are similar to the untreated surface. The author claimed that the reduced adhesion of platelets is due to surface chemistry instead of morphology because the difference on L- and H- patterns is negligible. The possible reasons are the presence of an oxidation layer and the increased hydrophilicity which reduced the adhesion of proteins on platelets. It is also be noticed that 98% coverage on H-patterns after 48 h could indicates the potential quick endotheli- alisation ability. Although this laser-textured surface did not show an increased adhesion and proliferation of HUVECs, but the ability to reduce platelets adhesion, and increased migration to increase the initial endothelialisation could also contribute benefits. DLIP technique could also make spots array structure on real stents with modified wettability [24], reduced platelet adhesion [135] and controlled drug releasing [136]. These functions make DLIP a highly potential technique to improve stents performance.

Direct laser ablation and DLIP techniques as well as other laser techniques are enough to produce various surface textures such as grooves, pillars, pores and more complex texture [137] thanks to their flexibility. Some of these features including grooves, pillars and pores has proved to be efficient for promotion of endothelialisation and pre- vention of in-stents restenosis in previously section, thus the patterns produced by laser should also be efficient. Chemistry modification during laser surface modification is another important factor to be considered since laser modification process could introduce heat effects and the reaction between materials and surrounding environment.

3.1.2. Laser induced periodic surface structure

Laser induced periodic surface structures (LIPSS) have much small interspaces between grooves and the grooves are not as neat as in con- ventional laser texturing. LIPSS usually happens in the vicinity of the laser ablation threshold [138], and their formation mechanism is com- plex. One possible explanation is that the ultra-fast laser irradiation cannot provide enough time for energy transfer from laser to lattice, and thin layer of surface is heated fast. When this layer reaches a metastable

condition, materials could be ablated through evaporation, non-thermal melting, fragmentation, and other processes. Combined with the influ- ence of laser-induced acoustic wave and polarisation of laser, the metastable surface then forms unique LIPSS structures on the, whose dimensions are much smaller than the wavelength used to manufacture them [139]. These unidirectional, irregular, nano to micron size grooved array surfaces closely simulate the topology of normal SMCs structure and can potentially promote endothelialisation, because ECs naturally grow on the extracellular matrix of intima with fibrous structures aligned with the direction of SMCs. Hence, LIPSS is a possibly excellent surface modification technique for stents.

Liang et al. [140] have fabricated LIPSS on 316L stainless steel stents by femtosecond laser (Fig. 12). The in vitro test indicated that the bio- mimetic structure selectively promoted proliferation of HUVECs while had no effect on the proliferation of vascular smooth muscle cells (VSMCs). The characterisation of hemocompatibility of the laser treated surfaces showed a low adhesion of platelets on lasered and untreated surface. *In vivo* test in rabbit confirmed the results of in vitro test: lasered surfaces had a good coverage of endothelialisation and neointimal hy- perplasia was only observed on the nontreated surface. Consequently, this completed comparison proved the efficiency of LIPSS on stents ap- plications thanks to the selective promotion of endothelialisation. It is also interesting to find some hierarchical structures which combined micron and nano size features by changing pulse energy and speed (Fig. 13), providing a hierarchical texture stimulation for cellular response. As stated in previous sections, these hierarchical surface structures have the potential for multi-functional surfaces. These find- ings also proved the achievability of complex texture by laser nano-texturing.

The work of Nozaki et al. [79] indicated the promoted proliferation of ECs on LIPSS surfaces. Specifically, hierarchical micro/nano LIPSS structures were created on Ni–Ti alloys (Fig. 14), promoting adhesion, proliferation, and orientation of ECs on the surface. A lower platelets adhesion was also achieved compared with as-polished surfaces and nano-LIPSS only surfaces. This hierarchical structure (micro/nano) showed increased hydrophobicity compared with nano-LIPSS surface
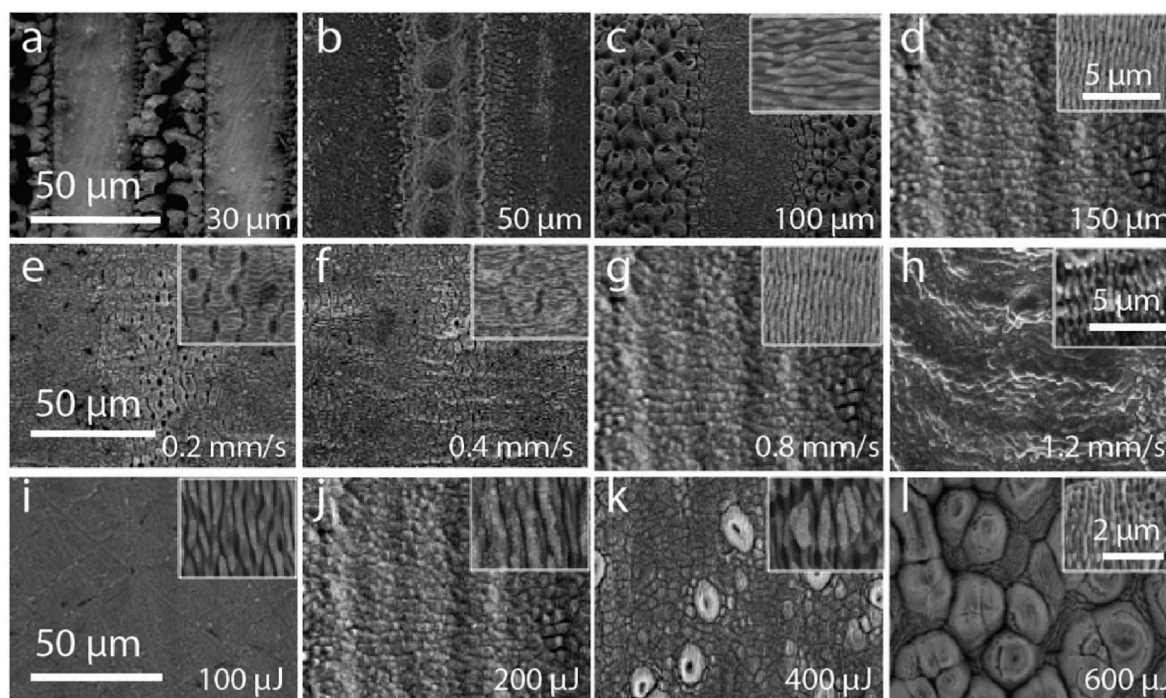

Fig. 12. Different surface structure created by laser at different condition: (a–d) different spot size at scanning speed of 0.8 mm/s and pulse energy at 200 μJ; (e–h) different feed speed at spot size of 150 μm and pulse energy at 200 μJ; (i–l) different pulse energy at spot size of 150 μm and feed speed at 0.8 mm/s, from Liang et al. [140].
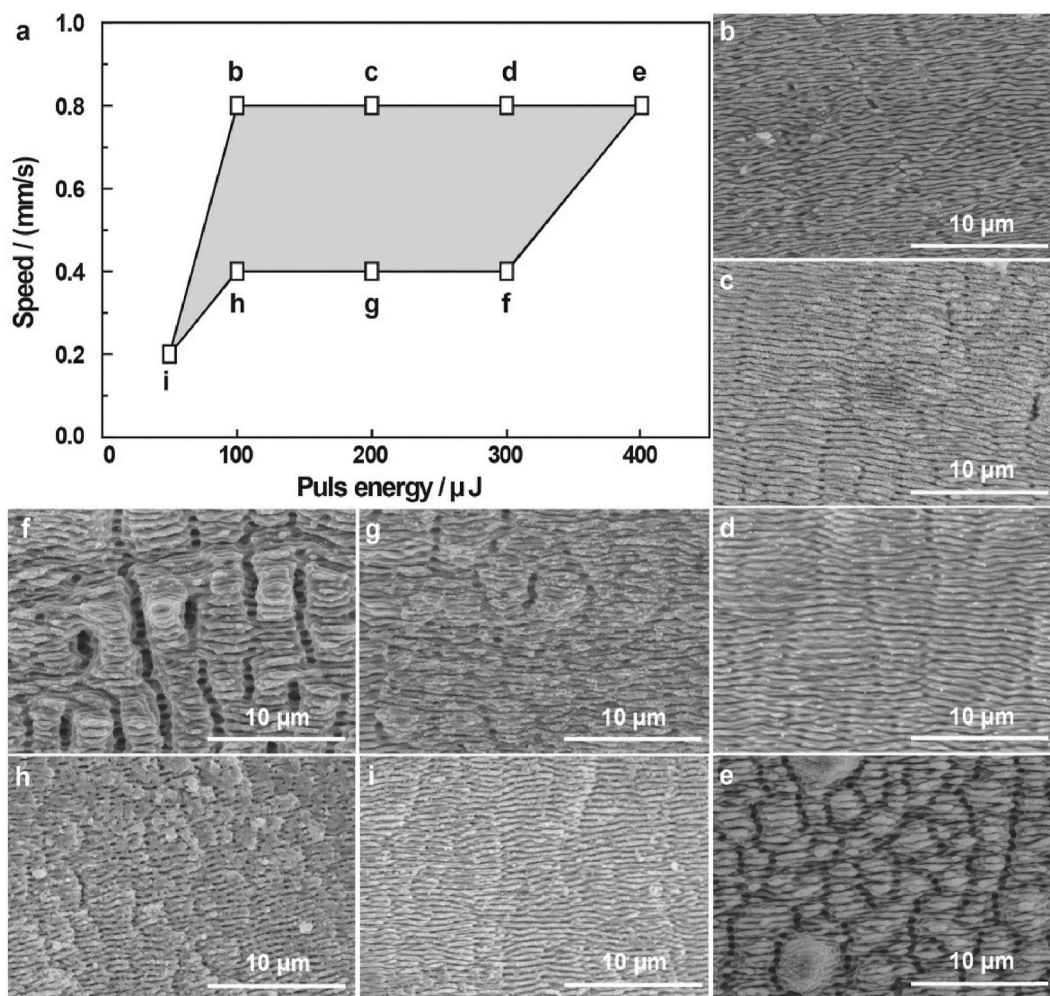
Fig. 13. LIPSS structure at different pulse energy and speed (a) Speed-Pulse energy plot for spot size 150 μm and (b–e) related SEM images, from Liang et al. [140].
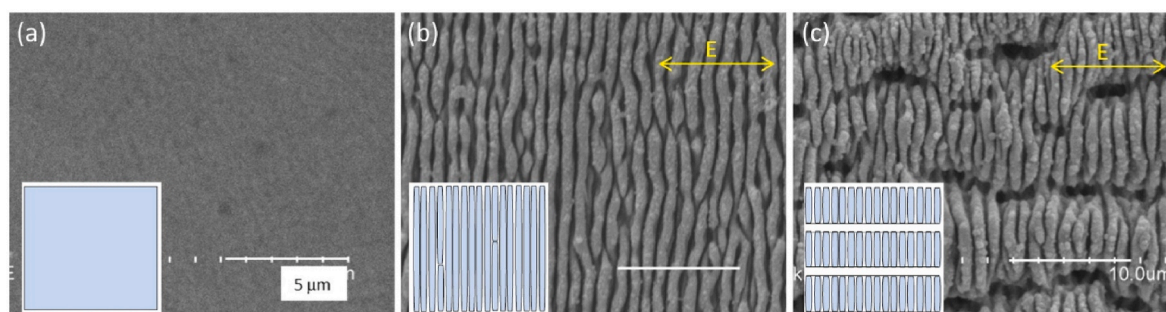

Fig. 14. Three types of LIPSS structures: (a) As-polished surface; (b) nano-LIPSS surface; (c) micro/nano LIPSS surface, from Nozaki et al. [79]. *E is the laser electric field polarisation vector. Scale bar (long white line) is 100 μm.*

and as-polished surfaces. And nano-LIPSS surfaces obtained an increase of hydrophilicity. It was proposed that the reason for different performance of platelets and ECs on LIPSS surface is the cell to structure size ratio. Platelets is around 2 μm as Fig. 15 shows and ECs is around 50–70 μm, micron grooves shown in Fig. 15c is around 2 μm which cannot provide enough ligand density to support platelets. Collectively, laser induced periodical surfaces with precisely controlled geometry pointed out again the huge influence of surface topography.

Hierarchical micro-nano LIPSS structures were also fabricated by Lin et al. [141]. They creatively utilised both linear and circular polarisation and fabricated circular, near-lattice-shaped LIPSS structures. Different

scanning speeds were also used for different size of micro-grooves (Fig. 16). The authors only used one condition (A1) to NIH3T3 fibroblast cells to evaluate cellular response, but the A1 LIPSS surface exhibited a greater cell density compared to the benchmark surfaces. It should be noticed that using circular polarisation in this research produced nano-size circular ripples and nano-features ("nanodots" in Fig. 16c). The change of circular polarisation provided another novel design for LIPSS textures and it is worth to check the cellular response for this circular nano-ripples as it might have different function because of the circular direction and "nanodots", which are similar to randomly roughened surface in nano to submicron range.
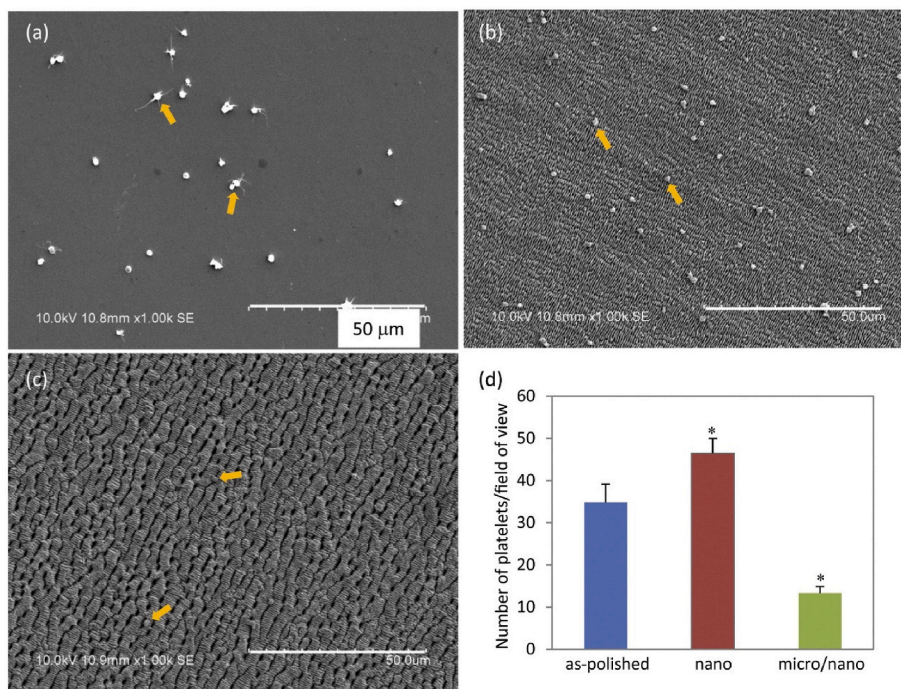
Fig. 15. Platelet adhesion on (a) as-polished; (b)nano-LIPSS; (c) micro/nano-LIPSS surface, from Nozaki et al. [79].
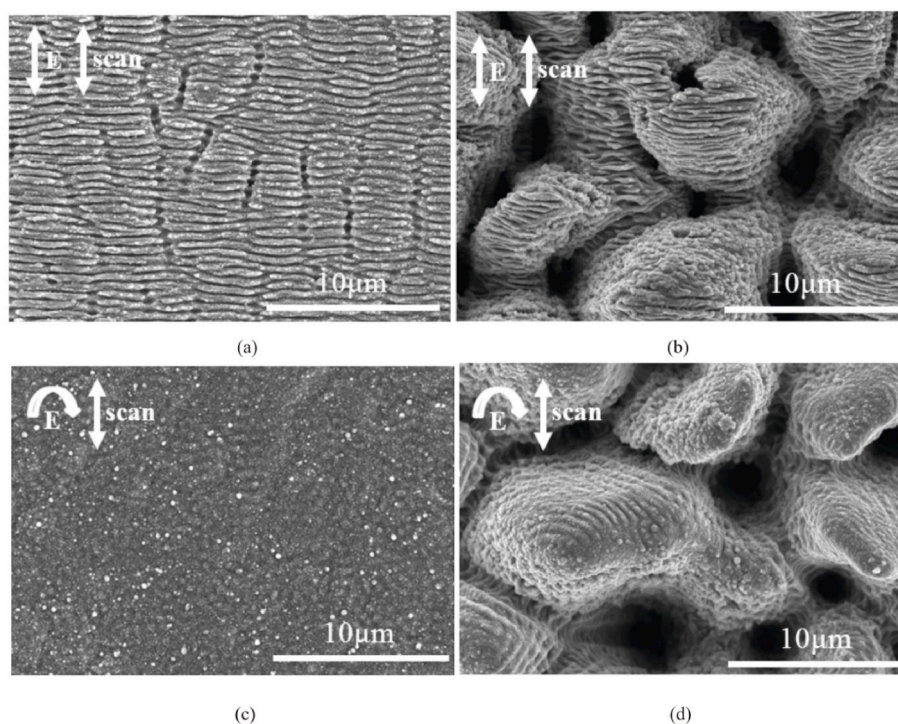

Fig. 16. FE-SEM images of different LIPSS surface structures (a) scanning speed is 2 mm/s; (b) scanning speed is 2 mm/s (c) scanning speed is 0.85 mm/s; (d) scanning speed is 0.85 mm/s. Laser fluence for all samples is 6.8 J/cm², from Lin et al. [141]. *E is the polarisation direction. Scan shows the direction of scanning direction.*

The function of LIPSS on stents goes beyond the promotion of endothelialisation. McDaniel et al. [142] revealed the prevention of monocyte proliferation on the LIPSS surface fabricated by Yb:KYW femtosecond laser. Two LIPSS structures with different periods and depths were fabricated on two types of stents made of 316L stainless steel (316L SS) and Pt:SS separately. Two types of cells were cultured on the surfaces, namely MS-5 fibroblasts and RAW 264.7 monocytes.

Fibroblast is essential for the formation of EC lumen [143] while monocyte is related to stents restenosis [144]. The usage of different wavelength fabricated different LIPSS surface with different periods and depths, these difference further lead to different cellular behaviours. On both laser-treated stents, monocytes exhibited poor adhesion on LIPSS surface, even exhibited apoptosis, compared with obvious clusters on untreated surface. While on 1030 nm treated LIPSS surface, fibroblast

exhibited health monolayers, which is hard to be observed on untreated surfaces. This results clearly indicated the promotion of growth of fibroblasts and prevention of monocytes on 1030 nm-LIPSS surface, further indicated the potential promotion of endothelialisation and prevention of restenosis of LIPSS surfaces. The different cellular behaviour on different LIPSS surface fabricated by laser with different wavelength also suggested the importance of texture dimension and the change of laser wavelength provided an idea to control LIPSS dimension.

Due to the similarity with biomimetic surface structures, LIPSS are an efficient surface texturing technique for promotion of endothelialisation, prevention of in-stents restenosis, and reduction of the adhesion of platelets. LIPSS can slow down the releasing of drug from drug-eluting stent according to the results of Sirolimus coated and LIPSS modified nitinol stents [145]. However, the differences of adhesion and proliferation ability between ECs and SMCs on LIPSS is not as much as other surface textures. For instance, a LIPSS surface after 24h cell culture shows around 50% more EC cells on the surface compared with the untreated surface [140], but for a grooved surface, the increase is circa 600%. Although the materials used in these two studies are not the same (316LSS and Ti, respectively), the comparison indicates that further improvement could be explored. Previous research dealt with the modification of the periodic [146] and size of LIPSS [147], their directions [148], and also the fabrication of LIPSS on polymers [149], even on biodegradable materials PLLA [150]. However more investigation should be done to optimise the suitable LIPSS structures for stent surface modifications.

3.2. Laser surface chemistry modification on stents and stent-related materials

Laser surface chemistry modification is also widely applied on many biodevices including stents. Laser surface nitridation is a popular laser surface chemistry modification due to the convenience of laser nitridation and efficiency of nitridation for improving biocompatibility.

3.2.1. Laser surface nitridation

Laser could also be utilised for surface nitridation of stents, which is also simpler than plasma surface nitridation. Laser gas nitridation (LGN) is a technique which utilises laser to process the surface in nitrogen. The concentration of nitrogen could be controlled with other inactive gases, such as argon, to produce different surfaces.

Li et al. [151] fabricated nitridated surface on Ti–6Al–4V alloy surface through diode LGN. They used a mixture of nitrogen and argon and found the higher fraction of nitrogen resulted in the higher surface hardness but also produced a nitridated layer with both longitude and transversal cracks. LGN process on 316L through CO_2 laser by Obeidi et al. [152] also produced the increasing hardness and wear resistance of surface after LGN. They also indicated that the increasing of harness is due to the increasing of martensite on the surface after LGN. Excimer laser was also used by Yue et al. [153] for LGN on 316LS stainless steel to produce nitridated surface without cracks. Reduced nickel ion releasing, increased corrosion and wear resistance was also found on the Nd-YAG LGN NiTi surface [154]. Additionally, increased biocompatibility [155], especially increased endothelialisation [151] were also found on surface of stent-related materials after LGN. The positive function of LGN on stents and stent-related materials is obviously proved. LGN also has drawbacks that it usually changes the surface topography and also induced a local thermal influence and stress on the surface. However, the application of LGN is still much more convenient than plasma surface nitridation methods, such as plasma physical [156] and chemical vapour deposition [157] and plasma-based ion implantation [158], because LGN does not need high temperature and high voltage during processing.

3.2.2. Laser surface oxidation

The function of oxidation on biological response is proved to be limited (as explained in details ins previous sections); however, oxidation by laser also can influence the degradation property in addition to topographical modifications. Donik et al. [159] investigated the degradation property of laser textured Fe–Mn alloy (Mn-18 wt%). The samples after laser treatment showed an increased degradation rate, which is the result of both increased oxidation content and surface areas. The oxidated metal acted as the trigger for further degradation, the combination with laser texturing, it could also achieve an enhanced degradability. This oxidation could be simply achieved by laser processing in air or oxygen, thus generally every laser machining such as laser etching, grinding, milling, texturing, cladding could be combined with oxidated surface. These flexibility and achievability are better than other surface modification methods.

3.2.3. Laser-based deposition techniques

Laser-assisted coating includes many coating techniques such as pulse laser deposition and laser chemical vapour deposition. Vapour can cover stents easily, hence vapour deposition is much suitable to coat the whole stents surface with complex 3D structures. Laser physical vapour deposition or pulsed laser deposition (PLD) is similar to other physical vapour deposition methods. It utilises laser as power source to evaporate target materials to coat the substrate. It should be noted that the target could be made of two/or more materials to obtain a composite coating on a substrate. Serbezov et al. [160] deposited DLC/Pt/Ag composite coating on both 316L SS and NiTi by PLD, resulting in the increasing corrosion resistance. The coating is 80 nm–120 nm in thickness and smooth, high quality without any cracks and droplets. Similar Ag and amorphous carbon composite coating was made, and the Ag nano-grains were found [153]. The advantage of PLD for coating is the high quality and even coating, and the temperature requirement for substrate and target is not as high as plasma physical vapour deposition. Processing temperature is important for some stent materials such as NiTi which is relatively sensitive to temperature. The alibility for nanocomposite coating fabrication is also noticeable, as nano composite usually provide unique cellular response, but the function needs to be further investigated. Laser chemical vapour deposition (LCVD) is also similar to other chemical vapour deposition methods for the deposition of metal and ceramic but use laser as power source. LCVD could be divided into two types: photolytic and pyrolytic, depending on the origin of reaction energy [161]. Kubová et al. [162] deposited hydrogenated amorphous carbon with extra oxygenic structures and conjugated double bonds on polytetrafluoroethylene (PTFE) by LCVD. The double bonds could origin from the acetylene ingredient and are photolytic results from triple bond. Further HUVEC culture showed the increased adhesion and proliferation on carbon coatings, indicating the potential application for stents coating. LCVD has potential for stents application with the advantages: it could achieve the flexible, tailorable, and selective surface coating, and also the chemical reaction could be selective with the help of different wavelength lasers. Laser vapour deposition still has disadvantages such as the limitation of coating area due to the limitation of laser power. However, laser vapour deposition is still suitable for stents due to the small size of stents. Combined with other advantages of laser, such as flexible, tailorable, selective and easy operation, laser vapour deposition is a high potential technique for stents surface coating.

3.3. Degradation control of biodegradable stent-related materials through laser

Main problems for polymeric BDSs are the large strut thickness, insufficient radial strength, and uncontrolled degradation. Materials for polymeric BDSs usually have low radial strength compared with DES which are the best therapeutic devices currently existing for coronary artery diseases. Thick struts are then necessary to provide enough support to BDSs but can cause further problems such as the disturbing of flood flow and slow endothelialisation. The First US Food and Drug Administration (FDA) approved BDSs are made by Abbott Vascular,

which are everolimus-eluting PLLA based BDSs and considered for potentially better performance than normal DESs [1]. But according to a 3-year clinical comparison with a cobalt-chromium everolimus-eluting stents in ABSORB III trial, this BDS has higher adverse event rates than DES [163]. Due to the poor clinical performance, several medical institutions worldwide issued the safety notice of this BDS and Abbott Vascular ABSORB BVS then voluntarily and permanently withdrew the stents in 2017. Since then, BDSs are under further investigations and one of the trends is to use metallic biodegradable materials as supporting structure. Some research investigated the bioresorbable metallic materials such as pure iron [164], magnesium [32] and zinc [165], these have higher modulus and strength compared with polymeric BDS materials. The problem for pure iron BDSs is the long degradation time, in fact still large portion of stents remains intact after 1 year as evidenced by *in vivo* study [164]. Magnesium BDS has instead relatively short degradation time, i.e., 4 months for full degradation [166]. Since coronary artery usually need 6-8-month for recovery [167], serving time of Mg BDS is not long enough for stents. Recently, another magnesium alloy has been used and been proven to be able to maintain the presence after 6 months [32]. Zinc is another novel BDS materials which shows promising performance within 1 year, as demonstrated by *in vivo* test [165]. There is also improvement for polymeric stents, National Medical Products Administration of China has approved a novel PLLA stent, NeoVas® bioabsorbable rapamycin-eluting stent (Lepu Medical Technology, China) in 2019 and the long term performance is proved by a comparison with CoCr DES [168]. MeRes™ (Meril Life Sciences, India) is another sirolimus bioresorbable PLLA stents which has a 100 μm strut thickness and the improved performance is also proved by 3 year follow-up [169]. Application of novel materials often need extra consideration in terms of selection of processing techniques used for forming and shaping, while laser surface treatments have the potential to be a universal solution to improve the surface strength and control the degradation.

3.3.1. Degradation control of biodegradable metallic stent-related materials through laser

Metallic biodegradable materials have high potential for stent applications because of their high strength, low inflammation, and relatively fast degradation compared to polymeric stents. But the degradation rate sometimes is not suitable to provide enough support time during the re-construction of coronary artery. The main purpose for laser surface modification is to control the degradation rate and increase the biocompatibility.

It is difficult for lasers to improve or modify the bulk strength of metallic BDS materials, but it is feasible for lasers to modify surface hardness and control the degradation rate. As magnesium-based and zinc-based BDSs usually possess the drawback of fast degradation rate, this could be adjusted by changing the composition of Mg alloy. Yet laser surface modification could be a processing technique which allows surface and localised physical and chemical modifications, which could be a potential solution to overcome the issue of degradation rate.

There are several types of biomedical bioresorbable Mg alloys, such as magnesium-zinc-dysprosium (Mg–Zn-Dy) and Magnesium–Zinc–Gallium (Mg–Zn-Ga). Rakesh et al. [170] employed LENS® MR-7 fibre laser system to carry out laser surface melting of Mg–1Zn-2Dy (wt%) alloys. Grooves structure with different dimension and surface roughness were fabricated on the surface. The hydrophobicity was increased due to the increased surface energy. Laser surface melting also increased the surface hardness, one reason is that laser induced rapid melting, evaporation, and cooling, thus refined the surface grains. Another reason is the pressure produced by the interaction of the involved vapour and laser. This pressure has the ability to make the surface denser and increase the surface hardness. Furthermore, laser surface melting also reduced the degradation rate, because of the changing surface phase content. As stated by Rakesh et al. [170], the corrosion mechanism of this alloy is filiform corrosion, which is caused

by surface defects and pits and then propagates to the bulk materials longitudinally. Increased surface grain density of secondary phase distributed along grain boundary reduces the anode to cathode area ratio (α-Mg to 2nd Mg phase), and as a result, corrosion of Mg alloy is decreased. Same function of reducing Mg alloy corrosion rate is found on femtosecond laser modified Mg–Ca–Zn alloys [171], increased surface hardness and reduced corrosion rate is also found in laser treated Zn–Zr alloys [172]. The refined grains and changed phase content or redistributed phase decreased the current corrosion and increased the corrosion potential. In conclusion, laser surface melting or laser surface modification can change the surface grain size and phase distribution and further affect surface hardness and corrosion rate.

3.3.2. Degradation control of biodegradable polymeric stent-related materials through laser

Controlled degradation is vital for the long-time *in vivo* performance of polymeric BDSs. Biodegradable polymers usually have slow degradation rate and long degradation time, leading to several problems for *in vivo* application. Since degradation mechanism of polymeric stents and metallic stents is different, controlled degradation is another challenge for laser surface modification of polymeric BDSs. Fig. 17 shows the degradation mechanism of semi-crystalline polymers. Semi-crystalline polymers have crystalline areas which are connected by amorphous areas. At the start of degradation, the amorphous areas firstly suffer chain scission, then the crystalline areas swell to create more amorphous regions, finally degradation occurs [167,173]. For amorphous polymers, the degradation mechanism is similar but without swelling of crystalline region. There are two main factors influencing the degradation process: crystallinity and molecular weight. Low crystallinity and low molecular weight could increase the degradation rate because the molecular structure is more susceptible to chain scission process. Hence the modification of the degradation properties of biodegradable polymers could be achieved by decreasing crystallinity and/or decreasing molecular weight to reduce the degradation rate.

The wavelength of laser is important for the degradation modification of polymeric biodegradable materials. Shibata et al. [174] compared the degradation difference using 800 nm and 400 nm fs lasers on PLGA. They fabricated three spots with similar diameters on PLGA by mechanical milling, 800 nm fs laser and 400 nm fs laser. The degradation data indicates that using a wavelength of 400 nm the laser processed pits had the fastest degradation rate; considering the result from XPS, FTIR and GPC, it might be because 400 nm laser is more efficient for bonds scission. However, the depths and morphology of three pits are not the same, therefore the effect of geometry should also be considered. It is hard to judge from SEM pictures (Fig. 18) as this had not been reported by the authors, but it seems that using a wavelength of 400 nm the pit shows the smallest depth while a wavelength of 800 nm results in pit with largest depth. Additionally, the pit processed at 400 nm is more porous although there are also some porous structures inside the pit produced by 800 nm laser. Deep pits have more surface than shallow pits, but the more porous structures achieved with a 400 nm laser provide additional surface area. This sub-feature might also contribute to the degradation of materials, and worth for more analysis such as wettability test to check the function of this nano-features. Stępak et al. [175] investigated the cross-section of PLLA after both 343 nm, 515 nm and 1030 nm laser irradiation. Compared with 343 nm and 515 nm laser, 1030 nm laser utilised in this experiment did not induce surface patterning, but there are many dots on the bottom surface of 1030 nm laser-treated surface. It is the result of the progression of filament inside the materials. As Fig. 19 shows, a molten layer was found at the laser ablation sides, and a filament layer is underneath the molten layer till the bottom, leading to the dots structure on the bottom surface. Filament layer was also found underneath the surface after laser irradiation at 515 nm, but not observed in the samples treated at 343 nm wavelength. They also repeated the same experiment on high crystallinity polymers, but no filament was visible. As claimed by the authors, this is because
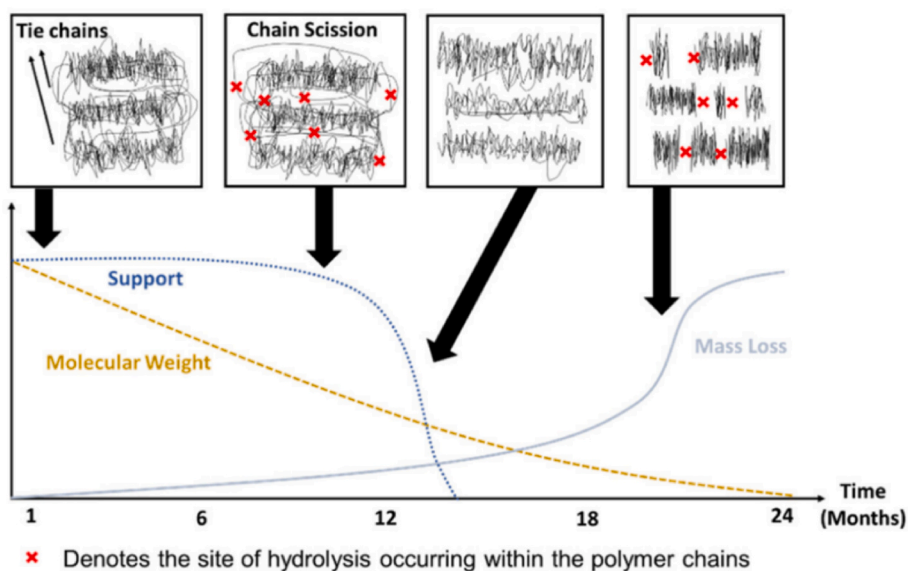
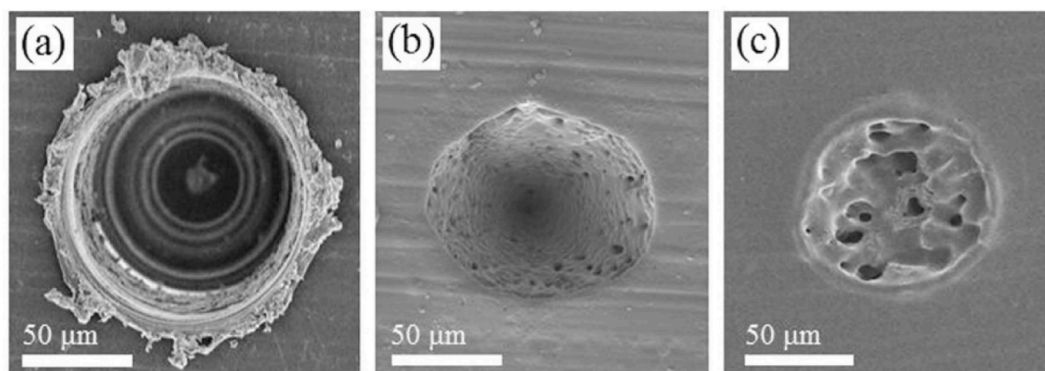**Fig. 17.** Chain scission degradation mechanism of biodegradable polymers plotted by Wee et al. [167].

Fig. 18. Crater fabricated on PLGA by Shibata et al. [174] *through (a) mechanical milling, (b)800 nm laser, (c)400 nm laser.*
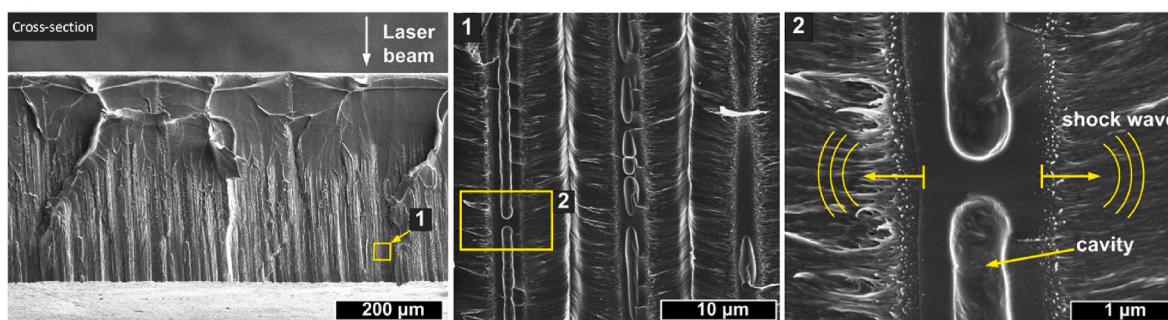

Fig. 19. The filament structure underneath the laser (1030 nm) treated surface from Stępak et al. [175].

this structure is created by self-focusing of laser inside PLLA during the transition of the laser, propagating the filaments. Because the crystals could change the light transition inside the materials, the filaments then cannot be found in samples with high crystallinity. Different pulse spacing has induced different filament density and structure underneath the surface of PLLA: large pulse spacing (such as 30 μs) has large filament density and more visible filament structure. Hence the density of filaments is adjustable by different laser parameters and also different crystallinity. The crystallization was also changed by these filaments because these filaments acted as crystallization nuclei, thus it is possible

to adjust the filaments by different laser irradiation and then adjust the crystallization behaviour, thereby achieving a control on mechanical and thermal properties. Additionally, further degradation result showed the increased degradation rate by these filaments. In conclusion, this filament structure provides a novel method to fabricated biodegradable polymeric materials with gradient mechanical, thermal properties with increased degradation rate, and has potential for stents applications.

The properties of the intrinsic materials such as crystallinity also need to be considered during laser process. Kryszak et al. [176] has utilised CO_2 laser (10.6 μm) to process the PLLA/HAp composite

extruded foils surfaces. One interesting change is the increased polymer distribution index (PDI), indicating the improved distribution of polymer molecular weight. Increased PDI proved that there are more short chains after laser irradiation, but still some larger chains with various molecular weight from low to high are present. When there are more short chains which are easy to crystallize, quick heating and cooling process does not provide enough time for crystallization, leading to the decreased crystallinity and further decrease of mechanical properties and faster degradation. And the DSC and WAXS results show clearly that the crystallinity was decreased by laser, additionally decreased molecular weight was observed in GPC and FTIR results. The mechanical properties of whole foil are also decreased, for some sample there is even 2 times decrease in Young's modulus. The decreased strength is not the expected change, thus the strength change during laser texturing of polymers should be carefully considered and more exploration should be done to maintain a reasonable strength of stents during laser texturing.

Laser surface modification of biodegradable materials for stents has been attracting increasing attention these years but there is no systematic analysis on the effect of wavelength, pulse width, and frequency on the degradation process, especially for polymeric biodegradable materials. There are still many challenges for improving strength and controlled degradation simultaneously, offering opportunities for future work in this field.

4. Future trends in laser surface engineering of stents

Future laser surface engineering for stent applications will need to consider simultaneously novel texturing and surface chemistry design. For example, Cui et al. [177,178] created a novel laser texturing design (Fig. 20). The combination of circle and linear scanning designs increased corrosion resistance on NiTi and increased bioactivity for osteoblast cells. In future different LIPSS designs will be employed to improve stents performance. By changing the polarisation direction (Skoulas et al. [23]) it will be possible to fabricate complex LIPSS

textures (Fig. 21) on stents. Furthermore, the employment of different rastering strategies at various pulse durations (Fraggelakis et al. [179]) will be need to be considered to apply novel designs (Fig. 22) on stents. Laser texturing in different gases could also be considered to introduce novel textures such as biomimetic surface structures, similar for example to the Lotus leaf created by Zorba et al. [180] through femtosecond laser irradiation under reactive SF_6 atmosphere (Fig. 23). It is also noticeable that laser could cross-link proteins to create 3D structure on the surface [181]. This technique could fabricate nano to micron textures and features on surfaces with different proteins including type I collagen mentioned in Section 2.2.1. This protein 3D texture on the surface has the potential to improve the biocompatibility of stents. Although these novel designs have not yet been designed for surface texturing of stents, these 3D freeform textures could potentially improve stents performance due to their nano and micrometric features and therefore careful consideration should be given in future research.

5. Conclusion

This critical review focused on state-of-the-art surface engineering and laser-based techniques to improve the performance of stents and stent-related materials leading to the following remarks:

- **Laser surface engineering has demonstrated potential to solve common problems found in stents.** Over the past decade stents have been successfully engineered in terms of materials development, surface modifications and structure optimisation, and the problems of LST and ISR have been addressed through design and development of novel materials and processing technologies. The modification of stents materials could solve the problems inherent to the previous generation of stents but further issues continuously arise with the introduction of new generations of stents. DESs solve the problems of high restenosis rate of BMSs but cause the late and very late in-stent restenosis problems; BDSs are striving to solve the late
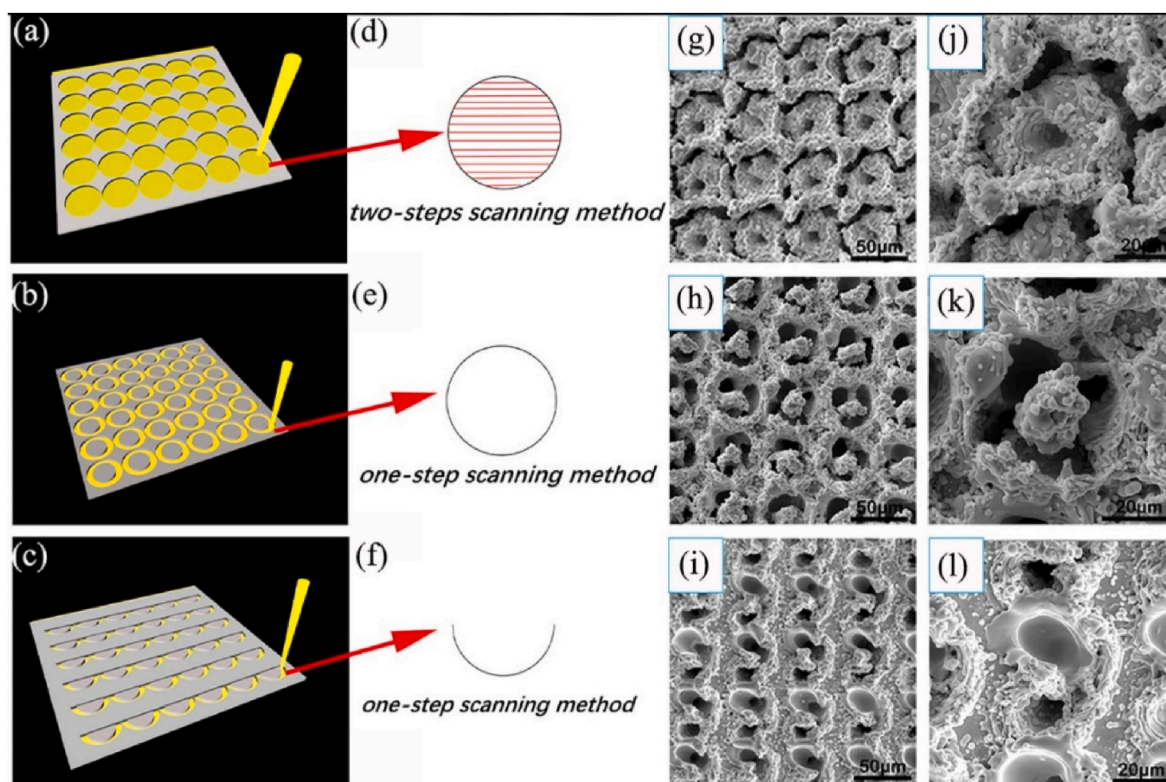

Fig. 20. Schematic and figures SEM images of three types of texture designs. (a) (d) (g) (j) two-steps: circle with grooves scanning; (b) (e) (h) (k) one-step circle scanning; (c) (f) (i) (l) on-step half circle scanning, from Li et al. [178].
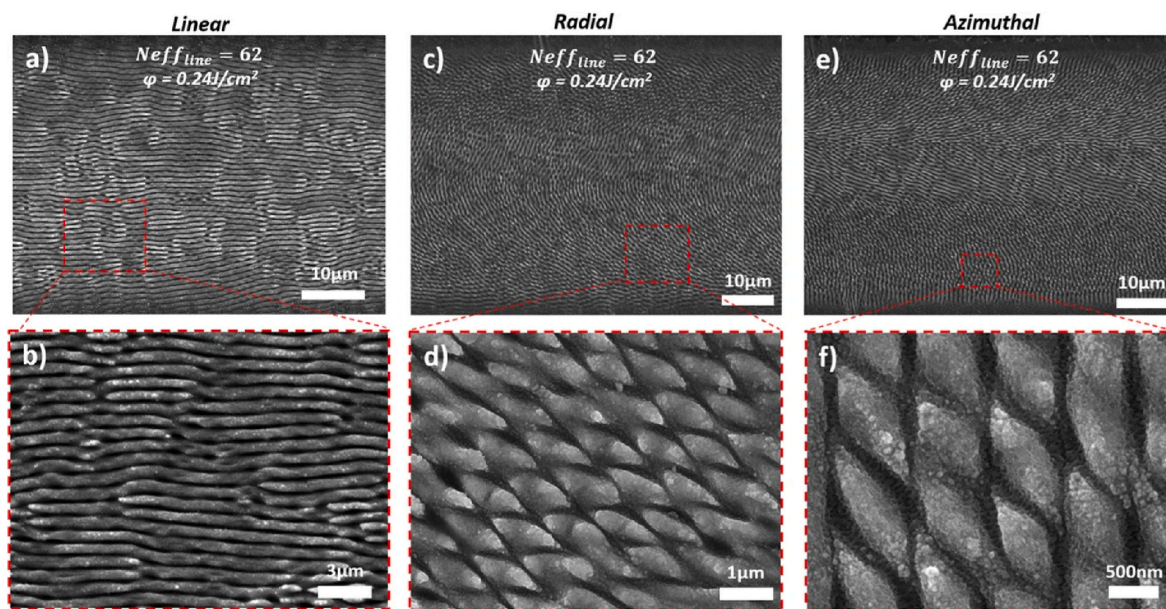
Fig. 21. SEM images of LIPSS produced at different polarisation conditions, replotted from Skoulas et al. [23].
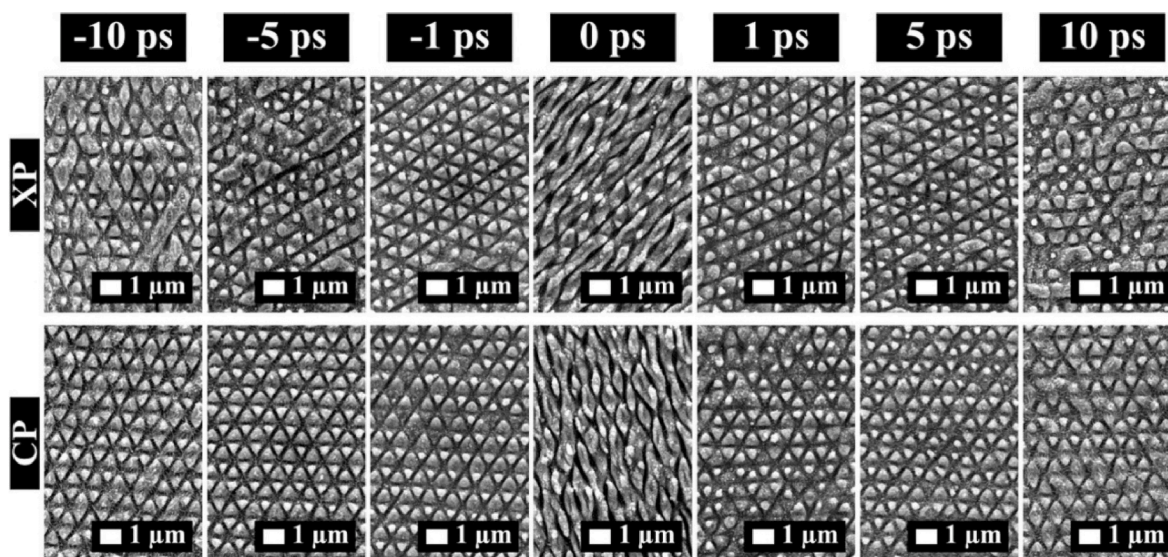

Fig. 22. SEM images of two scanning with different pulse delay from −10ps to 10ps. XP: cross-polarisation. CP: circular polarisation. Replotted from Fraggelakis et al. [179].

in-stent restenosis problem of DESs but lead to other restenosis problems related to low strength and degradation process. The challenging physiological environment of cardiovascular stents requires a balance of mechanical performance of stenting materials and also good hemocompatibility and biocompatibility, but surface modification of existing stents could have a huge impact on stent performance without affecting the bulk material properties. There are several commonly utilised surface modification techniques, including blasting, chemical etching, chemical vapour deposition, electrical discharge machining and plasma surface modification. However, these techniques are less suitable for stents than laser-based techniques because laser-based processes are easier, faster, more repeatable, and more tailorable than other processing techniques.

- **Laser-based techniques are suitable for surface modification of stents**, **however it is vital to understand the function of different texturing and surface chemistry for stent applications.** Based on the exploration of the influence of different surface textures and surface chemistry on stents, many surface textures including grooves, tubes, pores, wired and some combined surface structures exhibited improvement of stent performance at different extent. Nano to submicron features (around 500 nm to 2 μm) are preferable for EC attachment, proliferation, and migration, because the size of ECs is 50–70 μm and the features around 500 nm to 2 μm provide enough ligand density and attachment area for cells. Features below 500 nm could not provide enough area for cell attachment, and large features above 2 μm could not provide enough ligand density for cell growth and migration. Orientation of textures is also very important. Grooves and other directionally aligned features could induce the functionalisation of SMC, transforming SMC from epithelial-like to mesenchymal and then prohibit the proliferation of SMC. Different
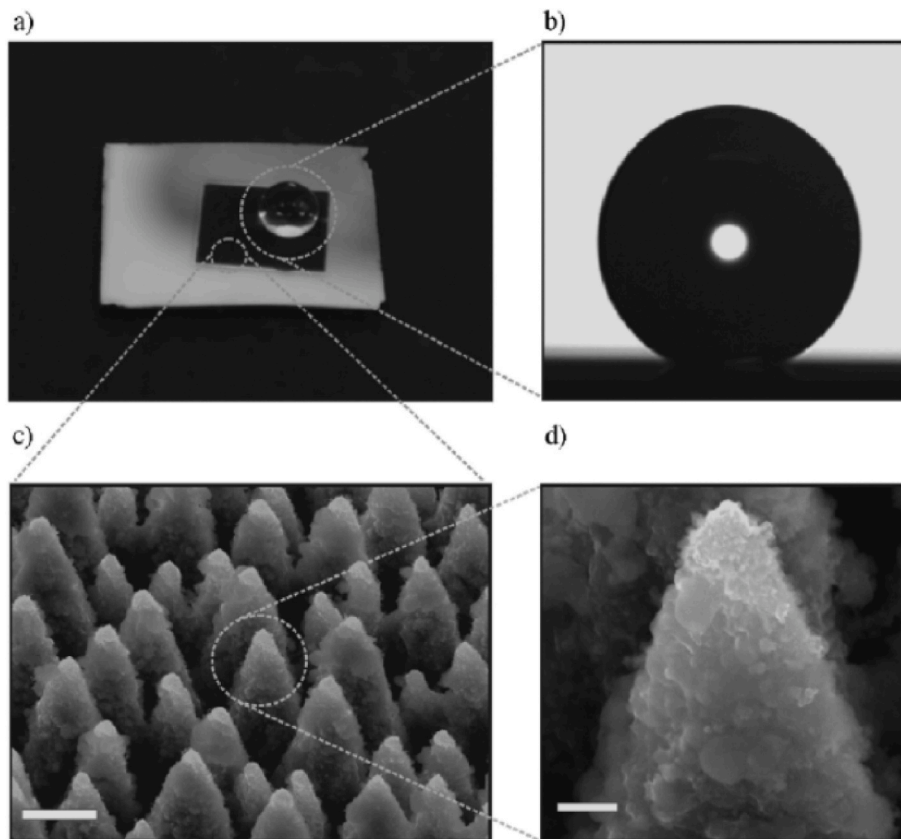
Fig. 23. Lotus leaf-like structure created by Zorba et al. through femtosecond laser irradiation under reactive SF$_6$ atmosphere [180].

surface chemistries should also be considered to design the ideal laser surface engineered structures on stents.

- **Surface chemistries including coatings and other surface functionalities strongly affect the stents performance.** The function of coatings is highly material-dependent. Laser-based processes can be successfully used to deposit various coatings on stents; however the complex set-up might be a drawback for scaling up the process in the biomedical industry. This review highlighted that the most useful surface chemistry is a nitrided one, as it can noticeably increase the biological response of EC and inhibit SMC attachment and proliferation as well as platelet adhesion.

- **Laser surface engineering provides a unique capability of combining micro/nano-texturing through preferential orientation while allowing nitridation of the surface locally.** Many laser-based techniques including direct laser patterning, LIPSS, laser surface nitridation and laser-assisted coatings have been proved to be able to improve stents performance. Direct laser patterning could make grooves and spots textures which could improve endothelialisation and reduce SMC proliferation. Combined with DLIP laser techniques, various texture design could be achieved and provide large flexibility for laser texturing of stents. In this context, LIPSS is a novel and potentially highly effective area of research. This special texture is a biomimetic structure and could promote endothelialisation, reduce SMC and platelet adhesion. LIPSS technique could also be expanded by multi-steps laser scanning and change of laser wavelength, polarisation condition, processing in different gas providing plenty of novel surfaces. Previous research proved the positive effects of laser surface texturing on stent-related materials, and the use of laser texturing on commercial stents and the *in vivo* test showed clearly the improved performance. Therefore, laser surface engineering can be employed to manufacture more suitable surfaces for stents applications while being effective in reducing adhesion of

platelets, promotion of endothelialisation and prevention of SMCs proliferation and migration.

- **Laser surface engineering can also modify the surface strength and provide a way to speed up or slow down the degradation for both metallic and polymeric BDSs.** However, laser surface modification on BDSs still need further investigation to fully understand the modification mechanism of laser on BDSs materials, which remains as an underexplored research gap within the biomedical field. BDS is a novel generation of stents which does not have a commercial materials solution, and related biodegradable materials are still under investigation. Nowadays, Mg alloy, Zn alloy, PLLA, PLGA and related copolymers are most utilised materials for BDSs. Laser surface engineering of these materials (or other novel BDS materials) to improve the biocompatibility and *in vivo* performance, enhance strength and control degradation process (either degradation rate or degradation steps) still does not have a systematic approach and solution. It is then worth for a deep exploration of laser surface engineering on BDSs.

- **Novel laser processing designs will provide various research direction for surface engineering of stents.** Although the function of novel laser processing designs on stents performance is still not investigated, those texturing and surface chemistry modifications by lasers have a strong potential to improve stents performance because of the combination of surface chemistry modifications and micro/nano-features manufacture. The understanding of the function of textures and surface chemistry is helpful for the design of novel textures.

Declaration of competing interest

The authors declare that they have no known competing financial interests or personal relationships that could have appeared to influence

the work reported in this paper.

References

[1] FDA Approves First Absorbable Stent for Coronary Artery Disease, FDA, (accessed Mar. 17, 2021), https://www.fda.gov/news-events/press-announcements/fda-approves-first-absorbable-stent-coronary-artery-disease.

[2] FDA Investigating Increased Rate of Major Adverse Cardiac Events Observed in Patients Receiving Abbott Vascular's Absorb GT1 Bioresorbable Vascular Scaffold (BVS) - Letter to Health Care Providers, FDA, https://www.fda.gov/medical-devices/letters-health-care-providers/fda-investigating-increased-rate-major-adverse-cardiac-events-observed-patients-receiving-abbott. (Accessed 17 March 2021).

[3] Class 1 device recall absorb bioresorbable vascular scaffold (BVS) system. https://www.accessdata.fda.gov/scripts/cdrh/cfdocs/cfRes/res.cfm?id=155009. (Accessed 17 March 2021).

[4] H.J. Rønold, S.P. Lyngstadaas, J.E. Ellingsen, A study on the effect of dual blasting with TiO2 on titanium implant surfaces on functional attachment in bone, J. Biomed. Mater. Res. 67 (2) (2003) 524–530, https://doi.org/10.1002/jbm.a.10580.

[5] H. Bretschneider, et al., Evaluation of topographical and chemical modified TiAl6V4 implant surfaces in a weight-bearing intramedullary femur model in rabbit, J. Biomed. Mater. Res. B Appl. Biomater. 108 (3) (2020) 1117–1128, https://doi.org/10.1002/jbm.b.34463.

[6] C.N. Elias, Y. Oshida, J.H.C. Lima, C.A. Muller, Relationship between surface properties (roughness, wettability and morphology) of titanium and dental implant removal torque, J. Mech. Behav. Biomed. Mater. 1 (3) (2008) 234–242, https://doi.org/10.1016/j.jmbbm.2007.12.002.

[7] A. Martin, M. König, H. Scheerer, G. Andersohn, M. Oechsner, Creation and description of sand blasted stamp created micro roughness on polyetheretherketone with subsequent physical vapor deposition coating for promotion of osseointegration, Mater. Werkst. 49 (11) (2018) 1301–1313, https://doi.org/10.1002/mawe.201700181.

[8] M. Kern, V.P. Thompson, Effects of sandblasting and silica-coating procedures on pure titanium, J. Dent. 22 (5) (Oct. 1994) 300–306, https://doi.org/10.1016/0300-5712(94)90067-1.

[9] G. Crisponi, et al., The meaning of aluminium exposure on human health and aluminium-related diseases, Biomol. Concepts 4 (1) (2013) 77–87, https://doi.org/10.1515/bmc-2012-0045.

[10] O. Sproesser, P.R. Schmidlin, J. Uhrenbacher, M. Roos, W. Gernet, B. Stawarczyk, Effect of sulfuric acid etching of polyetheretherketone on the shear bond strength to resin cements, J. Adhesive Dent. 16 (5) (2014) 465–472, https://doi.org/10.3290/j.jad.a32806.

[11] S.P. Sun, M. Wei, J.R. Olson, M.T. Shaw, Alkali etching of a poly(lactide) fiber, ACS Appl. Mater. Interfaces 1 (7) (2009) 1572–1578, https://doi.org/10.1021/am900227f.

[12] Z. Lei, H. Zhang, E. Zhang, J. You, X. Ma, X. Bai, Antibacterial activities and biocompatibilities of Ti-Ag alloys prepared by spark plasma sintering and acid etching, Mater. Sci. Eng. C 92 (2018) 121–131, https://doi.org/10.1016/j.msec.2018.06.024. June.

[13] L.F. He, J.G. Chen, DNA damage, apoptosis and cell cycle changes induced by fluoride in rat oral mucosal cells and hepatocytes, World J. Gastroenterol. 12 (7) (2006) 1144–1148, https://doi.org/10.3748/wjg.v12.i7.1144.

[14] R.M. Melo, R.O.A. Souza, E. Dursun, E.B.C. Monteiro, L.F. Valandro, M.A. Bottino, Surface treatments of zirconia to enhance bonding durability, Operat. Dent. 40 (6) (2015) 636–643, https://doi.org/10.2341/14-144-L.

[15] L. Minati, C. Migliaresi, L. Lunelli, G. Viero, M. Dalla Serra, G. Speranza, Plasma assisted surface treatments of biomaterials, Biophys. Chem. 229 (2017) 151–164, https://doi.org/10.1016/j.bpc.2017.07.003. July.

[16] W.M. Steen, J. Powell, Laser surface treatment, in: fourth ed., in: W.M. Steen, J. Powell (Eds.), Laser Materials Processing, vol. 2, Springer London, London, 2010, pp. 157–162, no. 3.

[17] M.C. Loya, K.S. Brammer, C. Choi, L.H. Chen, S. Jin, Plasma-induced nanopillars on bare metal coronary stent surface for enhanced endothelialization, Acta Biomater. 6 (12) (2010) 4589–4595, https://doi.org/10.1016/j.actbio.2010.07.007.

[18] W. Jin, P.K. Chu, Surface functionalization of biomaterials by plasma and ion beam, Surf. Coating. Technol. 336 (2018) 2–8, https://doi.org/10.1016/j.surfcoat.2017.08.011.

[19] M.N. Ramiasa, et al., Plasma polymerised polyoxazoline thin films for biomedical applications, Chem. Commun. 51 (20) (2015) 4279–4282, https://doi.org/10.1039/c5cc00260e.

[20] M. Loya, Design and Fabrication of Advanced Surface Microstructures : Surface Modification of Cardiovascular Stent Wires via RF Plasma Processing, 2010.

[21] P.K. Chu, J.Y. Chen, L.P. Wang, N. Huang, Plasma-surface modification of biomaterials, Mater. Sci. Eng. R Rep. 36 (5–6) (29-Mar-2002) 143–206, https://doi.org/10.1016/S0927-796X(02)00004-9. Elsevier Ltd.

[22] C. Tan, et al., Laser interference lithography, Adv. Nanotechnology. 4 (2010) 179–204.

[23] E. Skoulas, A. Manousaki, C. Fotakis, E. Stratakis, Biomimetic surface structuring using cylindrical vector femtosecond laser beams, Sci. Rep. 7 (2017) 1–11, https://doi.org/10.1038/srep45114. March.

[24] L. Gao, et al., Fabrication of hydrophobic structures on stent by direct three-beam laser interference lithography, Optik (Stuttg). 127 (13) (Jul. 2016) 5211–5214, https://doi.org/10.1016/j.ijleo.2016.02.075.

[25] M. Hamon, E. Lécluse, J.P. Monassier, G. Grollier, J.C. Potier, Pharmacological approaches to the prevention of restenosis after coronary angioplasty, Drugs Aging 13 (4) (1998) 291–301, https://doi.org/10.2165/00002512-199813040-00005.

[26] M. Félétou, "Multiple Functions of the Endothelial Cells - the Endothelium - NCBI Bookshelf," *the Endothelium: Part 1: Multiple Functions of the Endothelial Cells—Focus on Endothelium-Derived Vasoactive Mediators*, 2011 accessed Sep. 02, 2020, https://www.ncbi.nlm.nih.gov/books/NBK57148/.

[27] W.H. Frishman, R. Chiu, B.R. Landzberg, M. Weiss, Medical therapies for the prevention of restenosis after percutaneous coronary interventions, Curr. Probl. Cardiol. 23 (10) (Oct. 1998) 533–635, https://doi.org/10.1016/S0146-2806(98)80002-9.

[28] D.J. Kereiakes, et al., Usefulness of a cobalt chromium coronary stent alloy, Am. J. Cardiol. 92 (4) (Aug. 2003) 463–466, https://doi.org/10.1016/S0002-9149(03)00669-6.

[29] R.I.D. Elrdevruedeoh, et al., "TCT-226: CARE II 8 Month follow-up results with the CardioMind® 0.014" Sparrow® sirolimus-eluting nitinol stent system, J. Am. Coll. Cardiol. 56 (13) (Sep. 2010) B53, https://doi.org/10.1016/j.jacc.2010.08.251.

[30] S. Windecker, et al., Randomized comparison of a titanium-nitride-oxide-coated stent with a stainless steel stent for coronary revascularization - the TiNOX trial, Circulation 111 (20) (2005) 2617–2622, https://doi.org/10.1161/CIRCULATIONAHA.104.486647.

[31] S. McMahon, et al., Bio-resorbable polymer stents: a review of material progress and prospects, Prog. Polym. Sci. 83 (2018) 79–96, https://doi.org/10.1016/j.progpolymsci.2018.05.002.

[32] L. Mao, et al., A promising biodegradable magnesium alloy suitable for clinical vascular stent application, Sci. Rep. 7 (1) (Jun. 2017) 46343, https://doi.org/10.1038/srep46343.

[33] E. Mostaed, M. Sikora-Jasinska, J.W. Drelich, M. Vedani, Zinc-based alloys for degradable vascular stent applications, Acta Biomater. 71 (2018) 1–23, https://doi.org/10.1016/j.actbio.2018.03.005.

[34] K. Gutensohn, et al., In vitro analyses of diamond-like carbon coated stents: reduction of metal ion release, platelet activation, and thrombogenicity, Thromb. Res. 99 (6) (2000) 577–585, https://doi.org/10.1016/S0049-3848(00)00295-4.

[35] M. Unverdorben, et al., "Comparison of a silicon carbide-coated stent versus a noncoated stent in human beings: the Tenax versus Nir Stent Study's long-term outcome, Am. Heart J. 145 (4) (2003), https://doi.org/10.1067/mhj.2003.90.

[36] F.O. Obiweluozor, B. Maharjan, A. Gladys Emechebe, C.H. Park, C.S. Kim, Mussel-inspired elastic interpenetrated network hydrogel as an alternative for anti-thrombotic stent coating membrane, Chem. Eng. J. 347 (April) (2018) 932–943, https://doi.org/10.1016/j.cej.2018.04.098.

[37] S. Zimmermann, et al., Improved adhesion at titanium surfaces via laser-induced surface oxidation and roughening, Mater. Sci. Eng. A 558 (2012) 755–760, https://doi.org/10.1016/j.msea.2012.08.101.

[38] B.K. Nayak, M.C. Gupta, Self-organized micro/nano structures in metal surfaces by ultrafast laser irradiation, Opt Laser. Eng. 48 (10) (2010) 940–949, https://doi.org/10.1016/j.optlaseng.2010.04.010.

[39] J. Yong, et al., Femtosecond laser direct writing of porous network microstructures for fabricating super-slippery surfaces with excellent liquid repellence and anti-cell proliferation, Adv. Mater. Interfaces 5 (7) (2018), https://doi.org/10.1002/admi.201701479.

[40] T. Yanagida, K. Nagashima, H. Tanaka, T. Kawai, Mechanism of critical catalyst size effect on MgO nanowire growth by pulsed laser deposition, J. Appl. Phys. 104 (1) (2008), https://doi.org/10.1063/1.2937194.

[41] J. Reif, O. Varlamova, F. Costache, Femtosecond laser induced nanostructure formation: self-organization control parameters, Appl. Phys. Mater. Sci. Process 92 (4) (2008) 1019–1024, https://doi.org/10.1007/s00339-008-4671-3.

[42] L. De Bartolo, et al., Influence of membrane surface properties on the growth of neuronal cells isolated from hippocampus, J. Membr. Sci. 325 (1) (2008) 139–149, https://doi.org/10.1016/j.memsci.2008.07.022.

[43] J. Lu, C. Yao, L. Yang, T.J. Webster, Decreased platelet adhesion and enhanced endothelial cell functions on nano and submicron-rough titanium stents, Tissue Eng. 18 (13–14) (2012) 1389–1398, https://doi.org/10.1089/ten.tea.2011.0268.

[44] T.W. Chung, D.Z. Liu, S.Y. Wang, S.S. Wang, Enhancement of the growth of human endothelial cells by surface roughness at nanometer scale, Biomaterials 24 (25) (2003) 4655–4661, https://doi.org/10.1016/S0142-9612(03)00361-2.

[45] S. Choudhary, M. Berhe, K.M. Haberstroh, T.J. Webster, Increased endothelial and vascular smooth muscle cell adhesion on nanostructured titanium and CoCrMo, Int. J. Nanomed. 1 (1) (2006) 41–49, https://doi.org/10.2147/nano.2006.1.1.41.

[46] D. Khang, J. Lu, C. Yao, K.M. Haberstroh, T.J. Webster, The role of nanometer and sub-micron surface features on vascular and bone cell adhesion on titanium, Biomaterials 29 (8) (2008) 970–983, https://doi.org/10.1016/j.biomaterials.2007.11.009.

[47] C. Xu, F. Yang, S. Wang, S. Ramakrishna, In vitro study of human vascular endothelial cell function on materials with various surface roughness, J. Biomed. Mater. Res. 71 (1) (2004) 154–161, https://doi.org/10.1002/jbm.a.30143.

[48] K. Zhou, et al., Nano-micrometer surface roughness gradients reveal topographical influences on differentiating responses of vascular cells on biodegradable magnesium, Bioact. Mater. 6 (1) (2021) 262–272, https://doi.org/10.1016/j.bioactmat.2020.08.004.

[49] S.A. Biela, Y. Su, J.P. Spatz, R. Kemkemer, Different sensitivity of human endothelial cells, smooth muscle cells and fibroblasts to topography in the nano-micro range, Acta Biomater. 5 (7) (2009) 2460–2466, https://doi.org/10.1016/j.actbio.2009.04.003.

[50] J. Linneweber, P.M. Dohmen, U. Kerzscher, K. Affeld, Y. Nosé, W. Konertz, The effect of surface roughness on activation of the coagulation system and platelet adhesion in rotary blood pumps, Artif. Organs 31 (5) (2007) 345–351, https://doi.org/10.1111/j.1525-1594.2007.00391.x.

[51] S. Moradi, N. Hadjesfandiari, S.F. Toosi, J.N. Kizhakkedathu, S.G. Hatzikiriakos, Effect of extreme wettability on platelet adhesion on metallic implants: from superhydrophilicity to superhydrophobicity, ACS Appl. Mater. Interfaces 8 (27) (2016) 17631–17641, https://doi.org/10.1021/acsami.6b03644.

[52] P. Vandrangi, S.C. Gott, R. Kozaka, V.G.J. Rodgers, M.P. Rao, Comparative endothelial cell response on topographically patterned titanium and silicon substrates with micrometer to sub-micrometer feature sizes, PloS One 9 (10) (2014), https://doi.org/10.1371/journal.pone.0111465.

[53] J. Lu, M.P. Rao, N.C. MacDonald, D. Khang, T.J. Webster, Improved endothelial cell adhesion and proliferation on patterned titanium surfaces with rationally designed, micrometer to nanometer features, Acta Biomater. 4 (1) (2008) 192–201, https://doi.org/10.1016/j.actbio.2007.07.008.

[54] A. Khakbaznejad, B. Chehroudi, D.M. Brunette, Effects of titanium-coated micromachined grooved substrata on orienting layers of osteoblast-like cells and collagen fibers in culture, J. Biomed. Mater. Res. 70 (2) (2004) 206–218, https://doi.org/10.1002/jbm.a.30058.

[55] R. Kemkemer, S. Jungbauer, D. Kaufmann, H. Gruler, Cell orientation by a microgrooved substrate can be predicted by automatic control theory, Biophys. J. 90 (12) (2006) 4701–4711, https://doi.org/10.1529/biophysj.105.067967.

[56] S. Chang, et al., Phenotypic modulation of primary vascular smooth muscle cells by short-term culture on micropatterned substrate, PloS One 9 (2) (2014), https://doi.org/10.1371/journal.pone.0088089.

[57] Y. Ding, et al., Effects of microtopographic patterns on platelet adhesion and activation on titanium oxide surfaces, J. Biomed. Mater. Res. 101 (3) (2013) 622–632, https://doi.org/10.1002/jbm.a.34361.

[58] B.K. Li, I. Rodriguez, J. Zhou, Platelet adhesion studies on nanostructured poly (lactic-co-glycolic-acid)- carbon nanotube composite, J. Biomed. Mater. Res. 86 (2) (2008) 394–401, https://doi.org/10.1002/jbm.a.31605.

[59] K. Sadoul, New explanations for old observations: marginal band coiling during platelet activation, J. Thromb. Haemostasis 13 (3) (2015) 333–346, https://doi.org/10.1111/jth.12819.

[60] V.C. Bui, et al., Response of human blood platelets on nanoscale groove patterns: implications for platelet storage, ACS Appl. Nano Mater. 3 (7) (2020) 6996–7004, https://doi.org/10.1021/acsanm.0c01326.

[61] M.C. Loya, K.S. Brammer, C. Choi, L.H. Chen, S. Jin, Plasma-induced nanopillars on bare metal coronary stent surface for enhanced endothelialization, Acta Biomater. 6 (12) (2010) 4589–4595, https://doi.org/10.1016/j.actbio.2010.07.007.

[62] L. Csaderova, E. Martines, K. Seunarine, N. Gadegaard, C.D.W. Wilkinson, M. O. Riehle, A biodegradable and biocompatible regular nanopattern for large-scale selective cell growth, Small 6 (23) (2010) 2755–2761, https://doi.org/10.1002/smll.201000193.

[63] P.P. Lee, A. Cerchiari, T.A. Desai, Nitinol-based nanotubular coatings for the modulation of human vascular cell function, Nano Lett. 14 (9) (2014) 5021–5028, https://doi.org/10.1021/nl501523v.

[64] K.R. Milner, A.J. Snyder, C.A. Siedlecki, Sub-micron texturing for reducing platelet adhesion to polyurethane biomaterials, J. Biomed. Mater. Res. 76 (3) (2006) 561–570, https://doi.org/10.1002/jbm.a.30554.

[65] O.G. Simionescu, C. Romanitan, O. Tutunaru, V. Ion, O. Buiu, A. Avram, RF magnetron sputtering deposition of TiO2 thin films in a small continuous oxygen flow rate, Coatings 9 (7) (2019) 1–13, https://doi.org/10.3390/coatings9070442.

[66] P. Formentín, et al., Human aortic endothelial cell morphology influenced by topography of porous silicon substrates, J. Biomater. Appl. 30 (4) (2015) 398–408, https://doi.org/10.1177/0885328215588414.

[67] S.M. Casillo, A.P. Peredo, S.J. Perry, H.H. Chung, T.R. Gaborski, "Membrane pore spacing can modulate endothelial cell–substrate and cell–cell interactions, ACS Biomater. Sci. Eng. 3 (3) (Mar. 2017) 243–248, https://doi.org/10.1021/acsbiomaterials.7b00055.

[68] R. Wessely, et al., Inhibition of neointima formation by a novel drug-eluting stent system that allows for dose-adjustable, multiple, and on-site stent coating, Arterioscler. Thromb. Vasc. Biol. 25 (4) (2005) 748–753, https://doi.org/10.1161/01.ATV.0000157579.52566.ee.

[69] N. Ferraz, J. Carlsson, J. Hong, M.K. Ott, Influence of nanoporesize on platelet adhesion and activation, J. Mater. Sci. Mater. Med. 19 (9) (2008) 3115–3121, https://doi.org/10.1007/s10856-008-3449-7.

[70] M. Karlsson, A. Johansson, L. Tang, M. Boman, Nanoporous aluminum oxide affects neutrophil behaviour, Microsc. Res. Tech. 63 (5) (2004) 259–265, https://doi.org/10.1002/jemt.20040.

[71] C. Aktas, et al., Micro- and nanostructured Al 2O 3 surfaces for controlled vascular endothelial and smooth muscle cell adhesion and proliferation, Mater. Sci. Eng. C 32 (5) (2012) 1017–1024, https://doi.org/10.1016/j.msec.2012.02.032.

[72] A.M. Cherian, J. Joseph, M.B. Nair, S.V. Nair, V. Maniyal, D. Menon, Successful reduction of neointimal hyperplasia on stainless steel coronary stents by titania nanotexturing, ACS Omega 5 (28) (2020) 17582–17591, https://doi.org/10.1021/acsomega.0c02045.

[73] C.C. Mohan, et al., Stable titania nanostructures on stainless steel coronary stent surface for enhanced corrosion resistance and endothelialization, Adv. Healthc. Mater. 6 (11) (2017), https://doi.org/10.1002/adhm.201601353.

[74] Y. Shen, et al., Investigation of surface endothelialization on biomedical nitinol (NiTi) alloy: effects of surface micropatterning combined with plasma nanocoatings, Acta Biomater. 5 (9) (2009) 3593–3604, https://doi.org/10.1016/j.actbio.2009.05.021.

[75] F. Airoldi, et al., Comparison of diamond-like carbon-coated stents versus uncoated stainless steel stents in coronary artery disease, Am. J. Cardiol. 93 (4) (2004) 474–477, https://doi.org/10.1016/j.amjcard.2003.10.048.

[76] M. Jaganjac, et al., Oxygen-rich coating promotes binding of proteins and endothelialization of polyethylene terephthalate polymers, J. Biomed. Mater. Res. 102 (7) (2014) 2305–2314, https://doi.org/10.1002/jbm.a.34911.

[77] K. Kiefer, et al., Al2O3 micro- and nanostructures affect vascular cell response, RSC Adv. 6 (21) (2016) 17460–17469, https://doi.org/10.1039/c5ra21775j.

[78] M. Félétou, Chapter 1 introduction, in: The Endothelium: Part 1: Multiple Functions of the Endothelial Cells—Focus on Endothelium-Derived Vasoactive Mediators, Morgan & Claypool Life Sciences, San Rafael (CA), 2011.

[79] K. Nozaki, et al., Hierarchical periodic micro/nano-structures on nitinol and their influence on oriented endothelialization and anti-thrombosis, Mater. Sci. Eng. C 57 (2015) 1–6, https://doi.org/10.1016/j.msec.2015.07.028.

[80] P. Buijtenhuijs, et al., Tissue engineering of blood vessels: characterization of smooth-muscle cells for culturing on collagen-and-elastin-based scaffolds, Biotechnol. Appl. Biochem. 39 (2) (2004) 141, https://doi.org/10.1042/ba20030105.

[81] F. Zhang, et al., Synthesis and blood compatibility of rutile-type titanium oxide coated LTI-carbon, Sci. China Ser. C Life Sci. 41 (4) (1998) 400–405, https://doi.org/10.1007/BF02882740.

[82] S. Windecker, et al., Stent coating with titanium-nitride-oxide for reduction of neointimal hyperplasia, Circulation 104 (8) (2001) 928–933, https://doi.org/10.1161/hc3401.093146.

[83] P.A.L. Tonino, et al., "Titanium-Nitride-Oxide–Coated versus everolimus-eluting stents in acute coronary syndrome: the randomized TIDES-ACS trial, JACC Cardiovasc. Interv. 13 (14) (2020) 1697–1705, https://doi.org/10.1016/j.jcin.2020.04.021.

[84] P.O. Tuomainen, et al., Five-year clinical outcome of titanium-nitride-oxide-coated bioactive stents versus paclitaxel-eluting stents in patients with acute myocardial infarction: long-term follow-up from the TITAX AMI trial, Int. J. Cardiol. 168 (2) (2013) 1214–1219, https://doi.org/10.1016/j.ijcard.2012.11.060.

[85] V. Varho, et al., "Early vascular healing after titanium–nitride–oxide-coated stent versus platinum–chromium everolimus-eluting stent implantation in patients with acute coronary syndrome, Int. J. Cardiovasc. Imag. 32 (7) (2016) 1031–1039, https://doi.org/10.1007/s10554-016-0871-7.

[86] T. Pilgrim, et al., Comparison of titanium-nitride-oxidecoated stents with zotarolimus-eluting stents for coronary revascularization: a randomized controlled trial, JACC Cardiovasc. Interv. 4 (6) (2011) 672–682, https://doi.org/10.1016/j.jcin.2011.02.017.

[87] D. Carrié, et al., Does carbofilm coating affect in-stent intimal proliferation? A randomized trial comparing Rx multi-link penta and tecnic carbostent^TM stents, J. Intervent. Cardiol. 20 (5) (2007) 381–388, https://doi.org/10.1111/j.1540-8183.2007.00281.x.

[88] D. Antoniucci, et al., "Clinical and angiographic outcomes following elective implantation of the carbostent in patients at high risk of restenosis and target vessel failure," Catheter, Cardiovasc. Interv. 54 (4) (2001) 420–426, https://doi.org/10.1002/ccd.2004.

[89] D. Antoniucci, et al., Clinical and angiographic outcome after coronary arterial stenting with the carbostent, Am. J. Cardiol. 85 (7) (2000) 821–825, https://doi.org/10.1016/S0002-9149(99)00874-7.

[90] E. Pasquino, Carbofilrn : Present and Future Applications in Biomedical Devices, vol. 19, 1993, pp. 169–179.

[91] P.D. Maguire, et al., Mechanical stability, corrosion performance and bioresponse of amorphous diamond-like carbon for medical stents and guidewires, Diam. Relat. Mater. 14 (8) (2005) 1277–1288, https://doi.org/10.1016/j.diamond.2004.12.023.

[92] C. Hansi, A. Arab, A. Rzany, I. Ahrens, C. Bode, C. Hehrlein, "Differences of platelet adhesion and thrombus activation on amorphous silicon carbide, magnesium alloy, stainless steel, and cobalt chromium stent surfaces," Catheter, Cardiovasc. Interv. 73 (4) (2009) 488–496, https://doi.org/10.1002/ccd.21834.

[93] J.M. Schmehl, C. Harder, H.P. Wendel, C.D. Claussen, G. Tepe, "Silicon carbide coating of nitinol stents to increase antithrombogenic properties and reduce nickel release," Cardiovasc, Revascularization Med 9 (4) (2008) 255–262, https://doi.org/10.1016/j.carrev.2008.03.004.

[94] J. Lahann, D. Klee, H. Thelen, H. Bienert, D. Vorwerk, H. Höcker, Improvement of haemocompatibility of metallic stents by polymer coating, J. Mater. Sci. Mater. Med. 10 (7) (1999) 443–448, https://doi.org/10.1023/A:1008939400812.

[95] G.W. Stone, et al., Comparison of a polymer-based paclitaxel-eluting stent with a bare metal stent in patients with complex coronary artery disease: a randomized controlled trial, Jama 294 (10) (2005) 1215–1223.

[96] E. Camenzind, P.G. Steg, W. Wijns, Stent thrombosis late after implantation of first-generation drug-eluting stents: a cause for concern, Circulation 115 (11) (Mar. 2007) 1440–1455, https://doi.org/10.1161/CIRCULATIONAHA.106.666800.

[97] G. Schurtz, C. Delhaye, C. Hurt, H. Thieuleux, G. Lemesle, Biodegradable polymer biolimus-eluting stent (NOBORI®) for the treatment of coronary artery lesions: review of concept and clinical results, Med. Dev. Evid. Res. 7 (1) (2014) 35–43, https://doi.org/10.2147/MDER.S44051.

[98] J.R. Margolis, The Excel stent: a good DES, but can we really stop clopidogrel after 6 Months? JACC Cardiovasc. Interv. 2 (4) (2009) 310–311, https://doi.org/10.1016/j.jcin.2009.01.005.

[99] E. Tin Hay, et al., A novel drug-eluting stent using bioabsorbable polymer technology: two-year follow-up of the CURAMI registry, Int. J. Cardiol. 131 (2) (2009) 272–274, https://doi.org/10.1016/j.ijcard.2007.07.074.

[100] P. Vranckx, et al., Biodegradable-polymer-based, paclitaxel-eluting Infinnium stent: 9-Month clinical and angiographic follow-up results from the SIMPLE II prospective multi-centre registry study, EuroIntervention 2 (3) (2006) 310–317.

[101] J. Zandstra, Biocompatibility of Monodisperse Microspheres Composed of a Biodegradable poly(DL-Lactide-Peg)-B-poly(L-Lactide) Multiblock Copolymer, 2016.

[102] A.C. Abizaid, et al., "TCT-226: CARE II 8 Month follow-up results with the CardioMind® 0.014" Sparrow® sirolimus-eluting nitinol stent system, J. Am. Coll. Cardiol. 56 (13) (2010) B53, https://doi.org/10.1016/j.jacc.2010.08.251.

[103] P. Li, et al., Phospholipid-based multifunctional coating via layer-by-layer self-assembly for biomedical applications, Mater. Sci. Eng. C 116 (April) (2020) 111237, https://doi.org/10.1016/j.msec.2020.111237.

[104] J. Liu, et al., Biodegradable phosphorylcholine copolymer for cardiovascular stent coating, J. Mater. Chem. B 8 (24) (2020) 5361–5368, https://doi.org/10.1039/d0tb00813c.

[105] V.D. Bhat, B. Klitzman, K. Koger, G.A. Truskey, W.M. Reichert, Improving endothelial cell adhesion to vascular graft surfaces: clinical need and strategies, J. Biomater. Sci. Polym. Ed. 9 (11) (1998) 1117–1135, https://doi.org/10.1163/156856298X00686.

[106] M. Sgarioto, P. Vigneron, J. Patterson, F. Malherbe, M.D. Nagel, C. Egles, Collagen type I together with fibronectin provide a better support for endothelialization, Comptes Rendus Biol. 335 (8) (2012) 520–528, https://doi.org/10.1016/j.crvi.2012.07.003.

[107] A.S. Pandey, et al., Mechanisms of endothelial cell attachment, proliferation, and differentiation on 4 types of platinum-based endovascular coils, World Neurosurg 82 (5) (Nov. 2014) 684–695, https://doi.org/10.1016/j.wneu.2013.08.029.

[108] C.J. Panetta, et al., A tissue-engineered stent for cell-based vascular gene transfer, Hum. Gene Ther. 13 (3) (Feb. 2002) 433–441, https://doi.org/10.1089/10430340252792567.

[109] H. Qiu, et al., Biomimetic engineering endothelium-like coating on cardiovascular stent through heparin and nitric oxide-generating compound synergistic modification strategy, Biomaterials 207 (2019) 10–22, https://doi.org/10.1016/j.biomaterials.2019.03.033. March.

[110] I.H. Bae, I.K. Park, D.S. Park, H. Lee, M.H. Jeong, Thromboresistant and endothelialization effects of dopamine-mediated heparin coating on a stent material surface, J. Mater. Sci. Mater. Med. 23 (5) (2012) 1259–1269, https://doi.org/10.1007/s10856-012-4587-5.

[111] S.J. Lee, et al., Heparin coating on 3D printed poly (l-lactic acid) biodegradable cardiovascular stent via mild surface modification approach for coronary artery implantation, Chem. Eng. J. 378 (2019) 122116, https://doi.org/10.1016/j.cej.2019.122116. June.

[112] E. Delivopoulos, M.M. Ouberai, P.D. Coffey, M.J. Swann, K.M. Shakesheff, M.E. Welland, Serum protein layers on parylene-C and silicon oxide: effect on cell adhesion, Colloids Surf. B Biointerfaces 126 (2015) 169–177, https://doi.org/10.1016/j.colsurfb.2014.12.020.

[113] M. Zelzer, D. Albutt, M.R. Alexander, N.A. Russell, The role of albumin and fibronectin in the adhesion of fibroblasts to plasma polymer surfaces, Plasma Process. Polym. 9 (2) (2012) 149–156, https://doi.org/10.1002/ppap.201100054.

[114] S. Krajewski, et al., Preclinical evaluation of the thrombogenicity and endothelialization of bare metal and surface-Coated neurovascular stents, Am. J. Neuroradiol. 36 (1) (2015) 133–139, https://doi.org/10.3174/ajnr.A4109.

[115] Q. Lin, P. Yan, F. Qiu, X. Song, G. Fu, J. Ji, Heparin/collagen multilayer as a thromboresistant and endothelial favorable coating for intravascular stent, J. Biomed. Mater. Res. 96 A (1) (2011) 132–141, https://doi.org/10.1002/jbm.a.32820.

[116] S. Meng, et al., The effect of a layer-by-layer chitosan-heparin coating on the endothelialization and coagulation properties of a coronary stent system, Biomaterials 30 (12) (2009) 2276–2283, https://doi.org/10.1016/j.biomaterials.2008.12.075.

[117] G. Li, P. Yang, Y. Liao, N. Huang, Tailoring of the titanium surface by immobilization of heparin/fibronectin complexes for improving blood compatibility and endothelialization: an in vitro study, Biomacromolecules 12 (4) (2011) 1155–1168, https://doi.org/10.1021/bm101468v.

[118] GORE® TIGRIS® vascular stent gains FDA approval for treatment of peripheral artery disease | gore medical. https://www.goremedical.com/news/gore-tigris-vascular-stent-fda-approval. (Accessed 30 March 2021).

[119] H.J. Kang, D.J. Kim, S.J. Park, J.B. Yoo, Y.S. Ryu, Controlled drug release using nanoporous anodic aluminum oxide on stent, Thin Solid Films 515 (12) (2007) 5184–5187, https://doi.org/10.1016/j.tsf.2006.10.029.

[120] L. Li, N. Mirhosseini, A. Michael, Z. Liu, T. Wang, Enhancement of endothelialisation of coronary stents by laser surface engineering, Laser Surg. Med. 45 (9) (Nov. 2013) 608–616, https://doi.org/10.1002/lsm.22180.

[121] J.K.F.S. Braz, et al., Plasma nitriding under low temperature improves the endothelial cell biocompatibility of 316L stainless steel, Biotechnol. Lett. 41 (4–5) (2019) 503–510, https://doi.org/10.1007/s10529-019-02657-7.

[122] E. Czarnowska, et al., Structure and properties of nitrided surface layer produced on NiTi shape memory alloy by low temperature plasma nitriding, Appl. Surf. Sci. 334 (2015) 24–31, https://doi.org/10.1016/j.apsusc.2014.07.109.

[123] R.W.Y. Poon, et al., Formation of titanium nitride barrier layer in nickel-titanium shape memory alloys by nitrogen plasma immersion ion implantation for better corrosion resistance, Thin Solid Films 488 (1–2) (2005) 20–25, https://doi.org/10.1016/j.tsf.2005.04.002.

[124] T. Wierzchoń, E. Czarnowska, J. Morgiel, A. Sowińska, M. Tarnowski, A. Roguska, The importance of surface topography for the biological properties of nitrided diffusion layers produced on Ti6Al4V titanium alloy, Arch. Metall. Mater. 60 (3B) (2015) 2153–2159, https://doi.org/10.1515/amm-2015-0361.

[125] J.E. Barbato, E. Tzeng, Nitric oxide and arterial disease, J. Vasc. Surg. 40 (1) (2004) 187–193, https://doi.org/10.1016/j.jvs.2004.03.043.

[126] M.C. Frost, M.M. Reynolds, M.E. Meyerhoff, Polymers incorporating nitric oxide releasing/generating substances for improved biocompatibility of blood-contacting medical devices, Biomaterials 26 (14) (2005) 1685–1693, https://doi.org/10.1016/j.biomaterials.2004.06.006.

[127] Z. Yang, et al., Nitric oxide producing coating mimicking endothelium function for multifunctional vascular stents, Biomaterials 63 (2015) 80–92, https://doi.org/10.1016/j.biomaterials.2015.06.016.

[128] C.W. McCarthy, R.J. Guillory, J. Goldman, M.C. Frost, Transition-metal-Mediated release of nitric oxide (NO) from S-nitroso-N-acetyl-D-penicillamine (SNAP): potential applications for endogenous release of NO at the surface of stents via corrosion Products, ACS Appl. Mater. Interfaces 8 (16) (2016) 10128–10135, https://doi.org/10.1021/acsami.6b00145.

[129] Y.X. Leng, J. Wang, P. Yang, J.Y. Chen, N. Huang, "The adhesion and clinical application of titanium oxide film on a 316 L vascular stent, Surf. Coating. Technol. 363 (2019) 430–435, https://doi.org/10.1016/j.surfcoat.2018.12.021. December 2018.

[130] C. Trepanier, M. Tabrizian, L. Yahia, L. Bilodeau, D.L. Piron, Effect of modification of oxide layer on NiTi stent corrosion resistance, J. Biomed. Mater. Res. 43 (4) (1998) 433–440, https://doi.org/10.1002/(SICI)1097-4636(199824)43:4<433::AID-JBM11>3.3.CO;2-R.

[131] S. Kakinoki, K. Takasaki, A. Mahara, T. Ehashi, Y. Hirano, T. Yamaoka, Direct surface modification of metallic biomaterials via tyrosine oxidation aiming to accelerate the re-endothelialization of vascular stents, J. Biomed. Mater. Res. 106 (2) (2018) 491–499, https://doi.org/10.1002/jbm.a.36258.

[132] J. rui Wang, L. Yu, J. hua Shi, B. Wang, Y. Lv, J. Hao, In vitro biodegradation and mechanical characteristics of a novel biliary stent made of magnesium alloy, Chinese J. Tissue Eng. Res. 18 (25) (2014) 3980–3986, https://doi.org/10.3969/j.issn.2095-4344.2014.25.008.

[133] M. Oberringer, et al., Reduced myofibroblast differentiation on femtosecond laser treated 316LS stainless steel, Mater. Sci. Eng. C 33 (2) (2013) 901–908, https://doi.org/10.1016/j.msec.2012.11.018.

[134] R. Schieber, et al., Direct laser interference patterning of CoCr alloy surfaces to control endothelial cell and platelet response for cardiovascular applications, Adv. Healthc. Mater. 6 (19) (2017) 1–14, https://doi.org/10.1002/adhm.201700327.

[135] J. Wang, L. Gao, Y. Li, B. Liu, Experimental research on laser interference micro/nano fabrication of hydrophobic modification of stent surface, Laser Med. Sci. 32 (1) (2017) 221–227, https://doi.org/10.1007/s10103-016-2105-6.

[136] J. Wang, Y. Li, L. Gao, S. Wang, A. Mao, B. Liu, Preparation of the micro/nano structures of the biomimetic coating stent for loading MiRNA126 by four-beam laser interference, Optik (Stuttg) 128 (2017) 247–252, https://doi.org/10.1016/j.ijleo.2016.10.030.

[137] S. Alamri, et al., Quo Vadis Surface Functionalization: How Direct Laser Interference Patterning Tackle Productivity and Flexibility in Industrial Applications, 2019, p. 27, https://doi.org/10.1117/12.2514209. March 2019.

[138] J. Byskov-Nielsen, J.M. Savolainen, M.S. Christensen, P. Balling, Ultra-short pulse laser ablation of metals: threshold fluence, incubation coefficient and ablation rates, Appl. Phys. Mater. Sci. Process 101 (1) (2010) 97–101, https://doi.org/10.1007/s00339-010-5766-1.

[139] G. Lazzini, A.H.A. Lutey, L. Romoli, M. Allegrini, F. Fuso, Ultra-fast laser machining of stainless steel, J. Instrum. 15 (4) (2020), https://doi.org/10.1088/1748-0221/15/04/C04018.

[140] C. Liang, et al., Biomimetic cardiovascular stents for in vivo re-endothelialization, Biomaterials 103 (Oct. 2016) 170–182, https://doi.org/10.1016/j.biomaterials.2016.06.042.

[141] C.Y. Lin, C.W. Cheng, K.L. Ou, Micro/nano-Structuring of medical stainless steel using femtosecond laser pulses, Phys. Procedia 39 (2012) 661–668, https://doi.org/10.1016/j.phpro.2012.10.086.

[142] C. McDaniel, O. Gladkovskaya, A. Flanagan, Y. Rochev, G.M. O'Connor, In vitro study on the response of RAW264.7 and MS-5 fibroblast cells on laser-induced periodic surface structures for stainless steel alloys, RSC Adv. 5 (53) (2015) 42548–42558, https://doi.org/10.1039/c5ra04342e.

[143] A.C. Newman, M.N. Nakatsu, W. Chou, P.D. Gershon, C.C.W. Hughes, The requirement for fibroblasts in angiogenesis: fibroblast-derived matrix proteins are essential for endothelial cell lumen formation, Mol. Biol. Cell 22 (20) (2011) 3791–3800, https://doi.org/10.1091/mbc.E11-05-0393.

[144] F.M. Ucar, A potential marker of bare metal stent restenosis: monocyte count - to-HDL cholesterol ratio, BMC Cardiovasc. Disord. 16 (1) (2016) 1–7, https://doi.org/10.1186/s12872-016-0367-3.

[145] M. Buehler, P. Molian, Nanosecond laser induced periodic surface structures on drug elution profiles in stents, J. Med. Devices, Trans. ASME 6 (3) (2012) 1–10, https://doi.org/10.1115/1.4006539.

[146] T. Kobayashi, T. Wakabayashi, Y. Takushima, J. Yan, Formation behavior of laser-induced periodic surface structures on stainless tool steel in various media, Precis. Eng. 57 (April) (2019) 244–252, https://doi.org/10.1016/j.precisioneng.2019.04.012.

[147] H. Hikage, N. Nosaka, S. Matsuo, High-spatial-frequency periodic surface structures on steel substrate induced by subnanosecond laser pulses, APEX 10 (11) (2017) 112701, https://doi.org/10.7567/APEX.10.112701. Nov.

[148] M. Martínez-Calderon, et al., Surface micro- and nano-texturing of stainless steel by femtosecond laser for the control of cell migration, Sci. Rep. 6 (November) (2016) 1–10, https://doi.org/10.1038/srep36296.

[149] J. Heitz, B. Reisinger, M. Fahrner, C. Romanin, J. Siegel, V. Svorcik, Laser-induced periodic surface structures (LIPSS) on polymer surfaces, Int. Conf. Transparent Opt. Networks (2012) 1–4, https://doi.org/10.1109/ICTON.2012.6253723.

[150] S. Yada, M. Terakawa, Femtosecond laser induced periodic surface structure on poly-L-lactic acid, Opt Express 23 (5) (Mar. 2015) 5694, https://doi.org/10.1364/OE.23.005694.

[151] G. Li, X. Yao, R.J. Wood, J. Guo, Y. Shi, "Laser surface nitriding of Ti–6Al–4V alloy in nitrogen–argon atmospheres, Coatings 10 (10) (2020) 1–12, https://doi.org/10.3390/coatings10101009.

[152] M.A. Obeidi, E. McCarthy, D. Brabazon, Laser surface processing with controlled nitrogen-argon concentration levels for regulated surface life time, Opt Laser. Eng. 102 (2018) 154–160, https://doi.org/10.1016/j.optlaseng.2017.11.007. November 2017.

[153] T.M. Yue, J.K. Yu, H.C. Man, The effect of excimer laser surface treatment on pitting corrosion resistance of 316LS stainless steel, Surf. Coating. Technol. 137 (1) (2001) 65–71, https://doi.org/10.1016/S0257-8972(00)01104-X.

[154] Z.D. Cui, H.C. Man, X.J. Yang, Characterization of the laser gas nitrided surface of NiTi shape memory alloy, Appl. Surf. Sci. 208–209 (1) (2003) 388–393, https://doi.org/10.1016/S0169-4332(02)01414-9.

[155] C.H. Ng, et al., Enhancing the cell proliferation performance of NiTi substrate by laser diffusion nitriding, Surf. Coating. Technol. 309 (2017) 59–66, https://doi.org/10.1016/j.surfcoat.2016.11.008.

[156] J. Gerth, U. Wiklund, The influence of metallic interlayers on the adhesion of PVD TiN coatings on high-speed steel, Wear 264 (9–10) (2008) 885–892, https://doi.org/10.1016/j.wear.2006.11.053.

[157] S.H. Lee, B.J. Kim, H.H. Kim, J.J. Lee, Structural analysis of AlN and (Ti1-XAlX)N coatings made by plasma enhanced chemical vapor deposition, J. Appl. Phys. 80 (3) (1996) 1469–1473, https://doi.org/10.1063/1.363015.

[158] M. Sano, et al., Titanium nitride coating on implanted layer using titanium plasma based ion implantation, Nucl. Instrum. Methods Phys. Res. Sect. B Beam Interact. Mater. Atoms 148 (1–4) (1999) 37–41, https://doi.org/10.1016/S0168-583X(98)00872-6.

[159] Č. Donik, A. Kocijan, I. Paulin, M. Hočevar, P. Gregorčič, M. Godec, "Improved biodegradability of Fe–Mn alloy after modification of surface chemistry and topography by a laser ablation, Appl. Surf. Sci. 453 (May) (2018) 383–393, https://doi.org/10.1016/j.apsusc.2018.05.066.

[160] V. Serbezov, N. Reifart, F. Herbst, DLC films for stent applications, in: 2009 3rd Ict. Mediterr. Winter Conf, ICTON-MW, 2009, pp. 10–15, https://doi.org/10.1109/ICTONMW.2009.5385606, 2009.

[161] H. Alemohammad, E. Toyserkani, Laser-assisted additive fabrication of micro-sized coatings, Adv. Laser Mater. Process. Technol. Res. Appl. (2010) 735–762, https://doi.org/10.1533/9781845699819.7.735.

[162] O. Kubová, et al., Characterization and cytocompatibility of carbon layers prepared by photo-induced chemical vapor deposition, Thin Solid Films 515 (17) (2007) 6765–6772, https://doi.org/10.1016/j.tsf.2007.02.014.

[163] D.J. Kereiakes, et al., 3-Year clinical outcomes with everolimus-eluting bioresorbable coronary scaffolds: the ABSORB III trial, J. Am. Coll. Cardiol. 70 (23) (2017) 2852–2862, https://doi.org/10.1016/j.jacc.2017.10.010.

[164] M. Peuster, C. Hesse, T. Schloo, C. Fink, P. Beerbaum, C. von Schnakenburg, Long-term biocompatibility of a corrodible peripheral iron stent in the porcine descending aorta, Biomaterials 27 (28) (2006) 4955–4962, https://doi.org/10.1016/j.biomaterials.2006.05.029.

[165] H. Yang, et al., Evolution of the degradation mechanism of pure zinc stent in the one-year study of rabbit abdominal aorta model, Biomaterials 145 (2017) 92–105, https://doi.org/10.1016/j.biomaterials.2017.08.022.

[166] R. Erbel, et al., Temporary scaffolding of coronary arteries with bioabsorbable magnesium stents: a prospective, non-randomised multicentre trial, Lancet 369 (9576) (2007) 1869–1875, https://doi.org/10.1016/S0140-6736(07)60853-8.

[167] D.W.Y. Toong, et al., Bioresorbable polymeric scaffold in cardiovascular applications, Int. J. Mol. Sci. 21 (10) (May 2020) 3444, https://doi.org/10.3390/ijms21103444.

[168] Y. Han, et al., A randomized trial comparing the NeoVas sirolimus-eluting bioresorbable scaffold and metallic everolimus-eluting stents, JACC Cardiovasc. Interv. 11 (3) (2018) 260–272, https://doi.org/10.1016/j.jcin.2017.09.037.

[169] A. Seth, et al., Three-year clinical and two-year multimodality imaging outcomes of a thin-strut sirolimus-eluting bioresorbable vascular scaffold: MeRes-1 trial, EuroIntervention 15 (7) (2019) 607–614, https://doi.org/10.4244/eij-d-19-00324.

[170] R.K. R, S. Bontha, R.M. R, M. Das, V.K. Balla, Laser surface melting of Mg-Zn-Dy alloy for better wettability and corrosion resistance for biodegradable implant applications, Appl. Surf. Sci. 480 (2019) 70–82, https://doi.org/10.1016/j.apsusc.2019.02.167. October 2018.

[171] J. Park, et al., Corrosion behavior of biodegradable Mg-based alloys via femtosecond laser surface melting, Appl. Surf. Sci. 448 (2018) 424–434, https://doi.org/10.1016/j.apsusc.2018.04.088.

[172] Z. Wang, Q. Zhang, P. Guo, X. Gao, L. Yang, Z. Song, Effects of laser surface remelting on microstructure and properties of biodegradable Zn-Zr alloy, Mater. Lett. 226 (2018) 52–54, https://doi.org/10.1016/j.matlet.2018.04.112.

[173] Y. Onuma, P.W. Serruys, Bioresorbable scaffold: the advent of a new era in percutaneous coronary and peripheral revascularization? Circulation 123 (7) (2011) 779–797, https://doi.org/10.1161/CIRCULATIONAHA.110.971606.

[174] A. Shibata, S. Yada, M. Terakawa, Biodegradability of poly(lactic-co-glycolic acid) after femtosecond laser irradiation, Sci. Rep. 6 (May) (2016) 1–9, https://doi.org/10.1038/srep27884.

[175] B. Stępak, M. Gazińska, M. Nejbauer, Y. Stepanenko, A. Antończak, Diverse nature of femtosecond laser ablation of poly(L-lactide) and the influence of filamentation on the polymer crystallization behaviour, Sci. Rep. 9 (1) (2019) 1–12, https://doi.org/10.1038/s41598-019-39640-1.

[176] B. Kryszak, K. Szustakiewicz, B. Stępak, M. Gazińska, A.J. Antończak, Structural, thermal and mechanical changes in poly(L-lactide)/hydroxyapatite composite extruded foils modified by CO 2 laser irradiation, Eur. Polym. J. 114 (2019) 57–65, https://doi.org/10.1016/j.eurpolymj.2019.02.030. February.

[177] Z. Cui, et al., Surface analysis and electrochemical characterization on micro-patterns of biomedical Nitinol after nanosecond laser irradiating, Surf. Coating. Technol. 391 (April) (2020) 125730, https://doi.org/10.1016/j.surfcoat.2020.125730.

[178] S. Li, Z. Cui, W. Zhang, Y. Li, L. Li, D. Gong, Biocompatibility of micro/nanostructures nitinol surface via nanosecond laser circularly scanning, Mater. Lett. 255 (2019) 126591, https://doi.org/10.1016/j.matlet.2019.126591.

[179] F. Fraggelakis, G. Mincuzzi, J. Lopez, I. Manek-Hönninger, R. Kling, Controlling 2D laser nano structuring over large area with double femtosecond pulses, Appl. Surf. Sci. 470 (2019) 677–686, https://doi.org/10.1016/j.apsusc.2018.11.106. September 2018.

[180] V. Zorba, et al., Biomimetic artificial surfaces quantitatively reproduce the water repellency of a lotus leaf, Adv. Mater. 20 (21) (2008) 4049–4054, https://doi.org/10.1002/adma.200800651.

[181] D. Serien, K. Sugioka, Fabrication of three-dimensional proteinaceous micro- and nano-structures by femtosecond laser cross-linking, Opto-Electronic Adv. 1 (4) (2018) 1–18, https://doi.org/10.29026/oea.2018.180008.